MOLECULAR AND CELLULAR BIOLOGY, July 2005, p. 6178–6198 Vol. 25, No. 14
0270-7306/05/$08.00+0 doi:10.1128/MCB.25.14.6178–6198.2005

A Human T-Cell Lymphotropic Virus Type 1 Enhancer of Myc Transforming Potential Stabilizes Myc-TIP60 Transcriptional Interactions

Soumya Awasthi,[1] Anima Sharma,[1] Kasuen Wong,[1] Junyu Zhang,[1] Elizabeth F. Matlock,[1] Lowery Rogers,[1] Pamela Motloch,[1] Shigeki Takemoto,[2] Hirokuni Taguchi,[2] Michael D. Cole,[3] Bernhard Lüscher,[4] Oliver Dittrich,[4]† Hideaki Tagami,[5] Yoshihiro Nakatani,[5] Monnie McGee,[6] Anne-Marie Girard,[7] Luke Gaughan,[8] Craig N. Robson,[8] Raymond J. Monnat, Jr.,[9] and Robert Harrod[1]*

Laboratory of Molecular Virology, Department of Biological Sciences, Southern Methodist University, 334-DLS, 6501 Airline Drive, Dallas, Texas 75275-0376[1]; Department of Hematology and Respiratory Medicine, Kochi Medical School Hospital, Kohasu, Okocho, Nankoku, Kochi 783-8505, Japan[2]; Department of Pharmacology and Toxicology, Dartmouth University Medical School and the Norris Cotton Cancer Center, Hanover, New Hampshire 03755[3]; Abt. Biochemie und Molekularbiologie, Institute für Biochemie, Klinikum der RWTH, Pauwelsstrasse 30, 52057 Aachen, Germany[4]; Department of Cancer Biology, Dana-Farber Cancer Institute, Harvard Medical School, 1 Jimmy Fund Way, Boston, Massachusetts 02115[5]; Department of Statistical Science, Southern Methodist University, 3225 Daniels Avenue, Dallas, Texas 75275-0332[6]; Center for Gene Research and Biotechnology, Oregon State University, Corvallis, Oregon 97331[7]; School of Surgical Sciences, University of Newcastle upon Tyne Medical School, Framlington Place, Newcastle upon Tyne NE2 4HH, United Kingdom[8]; and Department of Pathology, University of Washington, Box 357705, Seattle, Washington 98195-7705[9]

Received 10 January 2005/Returned for modification 17 February 2005/Accepted 6 April 2005

The human T-cell lymphotropic virus type 1 (HTLV-1) infects and transforms CD4$^+$ lymphocytes and causes adult T-cell leukemia/lymphoma (ATLL), an aggressive lymphoproliferative disease that is often fatal. Here, we demonstrate that the HTLV-1 pX splice-variant p30^{II} markedly enhances the transforming potential of Myc and transcriptionally activates the human cyclin D2 promoter, dependent upon its conserved Myc-responsive E-box enhancer elements, which are associated with increased S-phase entry and multinucleation. Enhancement of c-Myc transforming activity by HTLV-1 p30^{II} is dependent upon the transcriptional coactivators, transforming transcriptional activator protein/p434 and TIP60, and it requires TIP60 histone acetyltransferase (HAT) activity and correlates with the stabilization of HTLV-1 p30^{II}/Myc-TIP60 chromatin-remodeling complexes. The p30^{II} oncoprotein colocalizes and coimmunoprecipitates with Myc-TIP60 complexes in cultured HTLV-1-infected ATLL patient lymphocytes. Amino acid residues 99 to 154 within HTLV-1 p30^{II} interact with the TIP60 HAT, and p30^{II} transcriptionally activates numerous cellular genes in a TIP60-dependent or TIP60-independent manner, as determined by microarray gene expression analyses. Importantly, these results suggest that p30^{II} functions as a novel retroviral modulator of Myc-TIP60-transforming interactions that may contribute to adult T-cell leukemogenesis.

The human T-cell lymphotropic virus type-1 (HTLV-1) infects CD4$^+$ T cells and causes adult T-cell leukemia/lymphoma (ATLL), an aggressive lymphoproliferative disease that is often fatal (59, 61, 65, 83). HTLV-1-infected leukemic lymphocytes exhibit deregulated cell cycle progression and characteristic multinucleation or polyploidy (evidenced by the appearance of flower-shaped or lobulated nuclei). A conserved sequence, known as pX, located within the 3′ terminus of the HTLV-1 genome, encodes at least five nonstructural regulatory factors, including the viral transactivator Tax and an alternative splice-variant, p30^{II} (or Tax open reading frame II [ORF II], Tof), which was shown to possess a functional transactivation domain (6, 13, 15, 29, 34, 35, 66, 86, 87). The pX sequence is generally retained in the majority of ATLL patient isolates, even those containing partially deleted proviruses (33, 68), indicative of its importance for pathogenesis.

The viral Tax protein transcriptionally activates numerous lymphoproliferative pathways (NF-κB, CREB/ATF, and p67^{SRF}) (29, 72, 73, 74, 75, 80, 84, 88) and has been shown to inhibit transcription functions associated with the tumor suppressor p53, which likely contributes to a loss of G_1/S-phase checkpoint control in HTLV-1-infected T cells (8, 46, 58). Many of the pleiotropic effects of Tax upon cellular signaling may derive from its aberrant recruitment of the transcriptional coactivators, p300/CREB-binding protein (p300/CBP) and p300/CBP-associated factor (P/CAF) (9, 22, 23, 27, 36, 37, 49, 50, 77, 78). Further, Tax interacts with cell cycle modulators, including D-type cylin-cdk4/6 complexes, retinoblastoma (Rb) protein, and the human mitotic arrest deficiency type 1

* Corresponding author. Mailing address: Laboratory of Molecular Virology, Department of Biological Sciences, Southern Methodist University, 334-DLS, 6501 Airline Drive, Dallas, TX 75275-0376. Phone: (214) 768-3864. Fax: (214) 768-3955. E-mail: rharrod@mail.smu.edu.

† Present address: Medizinische Hochschule Hannover, Institut für Pharmakologie, 30625 Hannover, Germany.

(hMAD-1) protein (21, 28, 31, 32, 39, 47, 52, 76). Although HTLV-1 Tax expression markedly promotes G_1/S transition (38, 40, 64), Tax has been demonstrated to inhibit Myc-dependent transactivation and prevent Myc-associated anchorage-independent cell growth (67). As ATLL patient-derived lymphocytes and tumors from HTLV-1 pX transgenic mice are known to possess deregulated Myc functions, these findings collectively suggest that other pX-encoded factors may influence Myc to promote cellular transformation by HTLV-1 (20, 43, 63).

The Myc transcription factor promotes S-phase cell cycle entry, induces apoptosis or programmed cell death, and causes neoplastic cellular transformation (2, 3, 7, 12, 19, 41, 51). The expression of the Myc protooncogene is deregulated in many solid tumors and hematological malignancies, including ATLL, diffuse large-cell lymphomas, $CD30^+$ anaplastic large-cell lymphomas, and Burkitt's B-cell lymphomas (18, 24, 26, 43, 55, 60). The transforming viruses, HTLV-1 and Epstein Barr virus, deregulate Myc functions associated with development of ATLL and Burkitt's lymphomas, respectively (11, 18, 26, 43, 63, 67). Our preliminary studies indicated that the HTLV-1 accessory protein $p30^{II}$ markedly increases S-phase cell cycle progression and induces significant polyploidy. As relatively little is known with respect to the roles of pX-encoded factors (e.g., $p30^{II}$, $p13^{II}$, $p12^{I}$, and Rex^{p27}) in HTLV-1-associated pathogenesis (6, 29, 34, 35), we sought to characterize the molecular mechanism by which $p30^{II}$ promotes Myc-dependent S-phase progression and multinucleation. While others have proposed that $p30^{II}$'s transcriptional functions are targeted against the viral LTR to repress HTLV-1 gene expression (1, 86, 87), the physiological role of $p30^{II}$ in ATLL-development remains unclear. Using microarray analyses, we now demonstrate that numerous cellular genes are transcriptionally activated by HTLV-1 $p30^{II}$ in a 60-kDa Tat-interacting protein (TIP60)-dependent or TIP60-independent manner. Nicot et al. (48) and Younis et al. (85) have shown that $p30^{II}$ binds and inhibits nuclear export of the doubly spliced Tax/Rex HTLV-1 mRNA, and it is intriguing that $p30^{II}$ might perform diverse functions to regulate viral gene expression and promote altered cellular growth, as has been noted for Tax, which drives LTR transactivation and deregulates host lymphoproliferative-signaling pathways (13, 21, 28, 29, 38, 40, 47, 52, 64, 72–76, 84). Robek et al. (62) have previously demonstrated that $p30^{II}$ is dispensable for immortalization and transformation of human peripheral blood mononuclear cells by an infectious HTLV-1 molecular clone, ACH.$p30^{II}$, which is defective for $p30^{II}$ production; however, the ACH.$p30^{II}$ mutant exhibited an approximately 20 to 50% reduction in transformation efficiency compared to the wild-type ACH.wt (62), suggesting that $p30^{II}$ is required for the full transforming potential of HTLV-1. Importantly, our findings indicate that HTLV-1 $p30^{II}$ is a novel retroviral modulator of Myc transcriptional and of transforming activities that may significantly contribute to adult T-cell leukemogenesis through stabilization of Myc-TIP60 transcriptional interactions.

MATERIALS AND METHODS

Plasmids, transfections, and cell culture. HeLa cells (ATCC CCL-2) were grown in Dulbecco's modified Eagle's medium (DMEM; ATCC) supplemented with 10% fetal bovine serum (FBS; Atlanta Biologicals), 100 U/ml penicillin, and 100 μg/ml streptomycin sulfate (Invitrogen-Life Technologies) and cultured at 37°C and 5% CO_2. 293A fibroblasts (Quantum Biotechnology) were cultured in ATCC 46-X medium supplemented with sodium bicarbonate (Invitrogen-Life Technologies), 10% FBS, and 100 U/ml penicillin and 100 μg/ml streptomycin sulfate. Molt-4 (ATCC CRL-1582), Jurkat E6.1 (ATCC TIB-152) and HTLV-1-infected MJ[G11] (ATCC CRL-8294) and HuT-102 lymphocytes (ATCC TIB-162) were grown in RPMI medium (ATCC) supplemented with 20% FBS, 100 U/ml penicillin, 100 μg/ml streptomycin sulfate, and 20 μg/ml gentamicin sulfate (Sigma Chemical Corp.) and cultured at 10% CO_2. Primary HTLV-1-infected lymphocytes were obtained after informed consent from three ATLL patients (ATL-1, ATL-2, ATL-3) and were cultured in RPMI medium supplemented with 20% FBS, 50 U/ml hIL-2 (Invitrogen-Life Technologies), 100 U/ml penicillin, 100 μg/ml streptomycin sulfate, and 20 μg/ml gentamicin sulfate. The cytomegalovirus (CMV)-HTLV-1 $p30^{II}$ (hemagglutinin [HA]) expression construct was kindly provided by G. Franchini (NCI, NIH) and has been reported by Koralnik et al. (34). pSG5-HTLV-1 $p13^{II}$ (10), which expresses a protein corresponding to amino acid residues 155 to 241 of HTLV-1 $p30^{II}$, was provided by V. Ciminale (University of Padua, Italy) and CMV-HTLV-1 $p13^{II}$ (HA) was provided by C. Nicot (University of Kansas). In order to generate the human cyclin D2 promoter-luciferase reporter construct, sequences encompassing the human cyclin D2 promoter were located in the clone with GenBank accession number U47284; according to these sequences, a PCR product that contains 1,622 nucleotides upstream of the ATG start codon was generated. Two closely spaced E-boxes (5′-CACGTG) are localized within the promoter region which binds Myc/Max/Mad network components (7). This fragment was cloned into the pGL3-luciferase vector. Both E-box sequences were mutated to 5′-CTCGAG using the quick change method. The M4-tk-luciferase (M4-tk-luc) reporter plasmid was reported by Bouchard et al. (7) and Vervoorts et al. (79). The CβF-FLAG-Myc, CβF-FLAG-$TRRAP_{1261\text{-}1579}$, CβS-$TRRAP_{antisense}$, and CβS constructs were described by McMahon et al. (41). The pOZ-wildtype-TIP60 and pOZ-$TIP60_{\Delta HAT}$ expression constructs were reported by Ikura et al. (25), and the CMV-$TIP60_{L497A}$ expression plasmid was reported by Gaughan et al. (17). All transfections were performed using Lipofectamine (Invitrogen-Life Technologies) or Superfect (QIAGEN) reagents as recommended by the manufacturers.

Cell cycle and fluorescence-activated cell sorter (FACS) analyses. Molt4 and Jurkat E6.1 lymphocytes were seeded in 100 mm^2 tissue culture dishes and transfected with CMV-HTLV-1 $p30^{II}$ (HA) or an empty CβS vector. After 48 h, cultures were split and either labeled for 4 h by adding BrdU (BD-Pharmingen) to the medium or immediately stained using annexin V-(fluorescein isothiocyanate [FITC])/propidium iodide (BD-Pharmingen). For cell cycle analyses, transfected BrdU-labeled cells were permeabilized and stained with a FITC-conjugated anti-BrdU antibody, and total genomic DNA was stained using 7-AAD (BD-Pharmingen). Flow cytometry was performed and data were analyzed using ModFit LT 3.0 software.

Focus formation/transformation assays. Immortalized Werner's Syndrome ($WRN^{-/-}$) fibroblasts (45) were seeded at 6×10^5 cells in 60 mm^2 tissue-culture dishes in DMEM supplemented with 10% FBS and cultured at 37°C under 5% CO_2. Cells were transfected with an empty CβS vector, CMV-HTLV-1 $p30^{II}$ (HA), CβF-FLAG-Myc, and combinations of CMV-HTLV-1 $p30^{II}$ (HA)/CβF-FLAG-Myc or CβS/CβF-FLAG-Myc using Superfect reagent. Foci were observed within 2 weeks and quantified by direct counting. Expression of HTLV-1 $p30^{II}$ (HA) was detected by fixing plates with 0.2% glutaraldehyde-1% formaldehyde in PBS and immunostaining using a monoclonal antibody against the HA epitope tag (CA5; Roche Molecular Biochemicals), diluted 1:1,000 in BLOTTO buffer (50 mM Tris-HCl [pH 8.0], 2 mM $CaCl_2$, 80 mM NaCl, 0.2% [vol/vol] NP-40, 0.02% [wt/vol] sodium azide, and 5% [wt/vol] nonfat dry milk). HTLV-1 $p30^{II}$ (HA) was visualized by immunofluorescence microscopy. $p30^{II}$-expressing fibroblast colonies were isolated and expanded in six-well tissue culture plates in DMEM supplemented with 10% FBS, 100 U penicillin, and 100 μg/ml streptomycin sulfate.

Immunoprecipitations and chromatin immunoprecipitation assays (ChIPs). Myc-interacting complexes were immunoprecipitated from transfected Jurkat E6.1 or HTLV-1-infected MJ[G11] and HuT-102 lymphocytes expressing HTLV-1 $p30^{II}$ (HA) using a monoclonal anti-HA tag antibody. Immunoprecipitation of endogenous $p30^{II}$ from cultured HTLV-1-infected ATLL patient-derived lymphocytes was performed using a rabbit polyclonal antibody against the COOH terminus of $p30^{II}$ (anti-HTLV-1 $p30^{II}$ antibody was generously provided by G. Franchini, NCI, NIH [34]). Briefly, 3×10^6 cells were harvested by centrifugation and lysed in RIPA buffer (1× PBS, 1% [vol/vol] IGEPAL CA-630, 0.5% sodium deoxycholate, and 0.1% sodium dodecyl sulfate [SDS]) containing the protease inhibitors bestatin, pepstatin, antipain dihydrochloride, chymostatin, and leupeptin (50 ng/ml each; Roche Molecular Biochemicals) followed by passage through a 27.5-gauge tuberculin syringe. Immunoprecipitations were

carried out by incubating precleared extracts with primary antibodies. Ten microliters of recombinant protein G-agarose (Invitrogen-Life Technologies) was added, and reactions were incubated with agitation at 4°C overnight. Matrices were pelleted by centrifugation at 6,500 rpm for 5 min and washed twice with RIPA buffer. Samples were resuspended in 40 μl 2× SDS-polyacrylamide gel electrophoresis loading buffer, and bound proteins were resolved by electrophoresis through 4 to 15% gradient or 12.5% Tris-glycine SDS-polyacrylamide gels. Chromatin-immunoprecipitations were performed using a kit from Upstate Biotechnology. Nucleoprotein complexes were cross-linked in vivo by adding 270 μl formaldehyde to approximately 3×10^6 Molt-4 or HTLV-1-infected MJ[G11] and HuT-102 lymphocytes in 100 mm^2 tissue-culture dishes for 10 min. Cells were pelleted by centrifugation and resuspended in 200 μl SDS lysis buffer. Chromatin DNA was fragmented by sonication, and oligonucleosomal-protein complexes were immunoprecipitated using primary antibodies and 60 μl salmon sperm DNA/protein A agarose. Precipitated oligonucleosomal-protein complexes were washed, cross-links were reversed, and bound DNA fragments were amplified by PCR using specific oligonucleotide primer pairs that flank conserved E-box elements within the human cyclin D2 gene promoter (PRM, 5′-CCCTTCCTCCTGGAGTGAAATAC-3′ and 5′-CGTGCTCTAACGCATCCTTGAGTC-3′) or anneal within an untranslated region (UTR, 5′-ATCAGACCCTATTCTCGGCTCAGG-3′ and 5′-CAGTCAGTAAGGCACTTTATTTCCCC-3′), as described by Vervoorts et al. (79). PCR products were electrophoresed through a 2% Tris-acetate-EDTA agarose gel and visualized by ethidium bromide staining.

RESULTS

HTLV-1 $p30^{II}$ increases S-phase progression and promotes polyploidy. The conserved pX domain of HTLV-1 encodes at least five nonstructural regulatory factors, including the viral transactivator Tax and an alternative splice variant, $p30^{II}$ (Fig. 1A). The HTLV-1 $p30^{II}$ protein is comprised of 241 amino acid residues and contains Arg- and Ser/Thr-rich domains (1, 34, 35). RasMol structural prediction analyses (Brookhaven protein databank) indicate that $p30^{II}$ possesses 4 alpha-helices and 19 beta-sheet regions (Fig. 1B). The alpha-helices likely serve as interacting or docking sites for cellular factors, whereas the Ser/Thr-rich domains may provide targets for phosphorylation by kinases that modulate $p30^{II}$'s functions or interactions. As relatively little is known with respect to the functions of HTLV-1 pX accessory factors, such as $p30^{II}$, we investigated whether the $p30^{II}$ protein contributes to lymphoproliferation in HTLV-1-infected T cells by altering cell cycle regulation. To determine whether HTLV-1 $p30^{II}$ influences cell cycle progression and/or apoptosis, Molt-4 and Jurkat E6.1 lymphocytes were transfected with a CMV-HTLV-1 $p30^{II}$ (HA) expression construct or an empty CβS vector control, and transfected cultures were assayed for bromodeoxyuridine (BrdU)-incorporation/cell cycle progression or programmed cell death using flow cytometric analyses (Fig. 1C and D and data not shown). HTLV-1 $p30^{II}$-expressing cells exhibit markedly increased S-phase progression and significant polyploidy as determined by BrdU incorporation and 7-AAD staining of total genomic DNA (Fig. 1C and D, top left panels). However, $p30^{II}$ did not induce apoptosis in transfected cells, as determined by annexin V-FITC/propidium iodide-staining and FACS (Fig. 1C and D, top right panels). These results suggest that $p30^{II}$ may contribute to lymphoproliferation and genomic instability in HTLV-1-infected cells during ATLL by affecting S-phase regulatory factors, such as Myc and/or E2F (2, 29, 43).

The HTLV-1 $p30^{II}$ protein interacts in Myc-TIP60 immune complexes in ATLL patient lymphocytes. The $p30^{II}$ protein was detected in cultured HTLV-1-infected lymphocytes, derived from three different ATLL patients (ATL-1, ATL-2, ATL-3) diagnosed with clinical acute-stage leukemias, by immunofluorescence laser confocal microscopy and immunoblotting (Fig. 2A and B). Three-dimensional Z-stack composite images for ATL-3 demonstrate that $p30^{II}$/Myc proteins colocalize in the nucleus in all focal planes in HTLV-1-infected cells (Fig. 2A, right panels). Relative fluorescence intensities for $p30^{II}$/Myc-specific signals and DAPI (4′,6′-diamidino-2-phenylindole) nuclear staining are shown for reference (Fig. 2A, right panels). HTLV-1 $p30^{II}$ is present in Myc-containing immunoprecipitated complexes in ATLL patient lymphocytes (Fig. 2B). Intriguingly, immunoprecipitation of Myc revealed that TIP49 (RUVBL1), TIP48 (RUVBL2) (81), and Max are present and are bound to Myc, but the TIP60 histone acetyltransferase (HAT) was not detected in Myc-containing coimmune complexes in uninfected Jurkat E6.1 lymphocytes (Fig. 2B). The NH_2 terminus of Myc is essential for Myc-dependent transformation and apoptosis-inducing functions and contains two conserved Myc homology domains (Myc box I [MBI] and MBII, respectively) that interact with cellular factors (2, 3, 7, 41, 42, 51, 81). The transcriptional coactivator, TRRAP/p434, and the ATPases/helicases, TIP49 (RUVBL1) and TIP48 (RUVBL2), interact with amino acids within MBII (41, 81). To determine if HTLV-1 $p30^{II}$ interacts with known Myc-binding partners, we transfected Jurkat E6.1 lymphocytes or HTLV-1-infected Hut-102 and MJ[G11] lymphocytes with CMV-HTLV-1 $p30^{II}$ (HA) or an empty CβS vector control and performed coimmunoprecipitations using a monoclonal anti-HA antibody (CA5; Roche Molecular Diagnostics). As shown in Fig. 2C, HTLV-1 $p30^{II}$ (HA) coimmunoprecipitates with Myc, TRRAP, TIP60, and TIP49 (RUVBL1). However, TIP48 (RUVBL2) and RNA polymerase II were not detected in anti-HA immunoprecipitates, although both proteins were detected in control immunoprecipitations using antibodies against known interacting proteins (Fig. 2C). To further confirm these interactions, we reimmunoprecipitated HTLV-1 $p30^{II}$ (HA) from extracts prepared from transfected Jurkat T cells using antibodies against Myc, TRRAP, TIP60, TIP48, and TIP49 (Fig. 2C, lower panels). A nonspecific antibody (rabbit preimmune serum) was included as a negative control. Interestingly, the ATPase/helicase, TIP48, was detected in $p30^{II}$-complexes immunoprecipitated with an anti-TIP48 (RUVBL2) polyclonal antibody (Fig. 2C, lower panels) (81). These data suggest that HTLV-1 $p30^{II}$ may modulate Myc functions through interactions with Myc-associated transcriptional coactivators on promoters of responsive genes (14).

HTLV-1 $p30^{II}$ transactivates Myc-responsive E-box elements within the human cyclin D2 promoter. To investigate the possibility that HTLV-1 $p30^{II}$ might affect Myc-dependent transcription, we next cotransfected HeLa cells with a human cyclin D2 promoter-luciferase reporter construct, containing two conserved Myc-responsive E-box enhancer elements (CACGTG), in the presence of increasing amounts of CMV-HTLV-1 $p30^{II}$ (HA). Results in Fig. 3A demonstrate that HTLV-1 $p30^{II}$ significantly transactivates the human cyclin D2 promoter. A mutant cyclin D2 promoter, lacking Myc-responsive E-box elements (79), was not transcriptionally activated by $p30^{II}$, indicating that $p30^{II}$-mediated transactivation from the human cyclin D2 promoter requires the conserved Myc-responsive E-box enhancer elements (Fig. 3A and B). The HTLV-1 $p30^{II}$ (HA)-tagged protein was detected in trans-

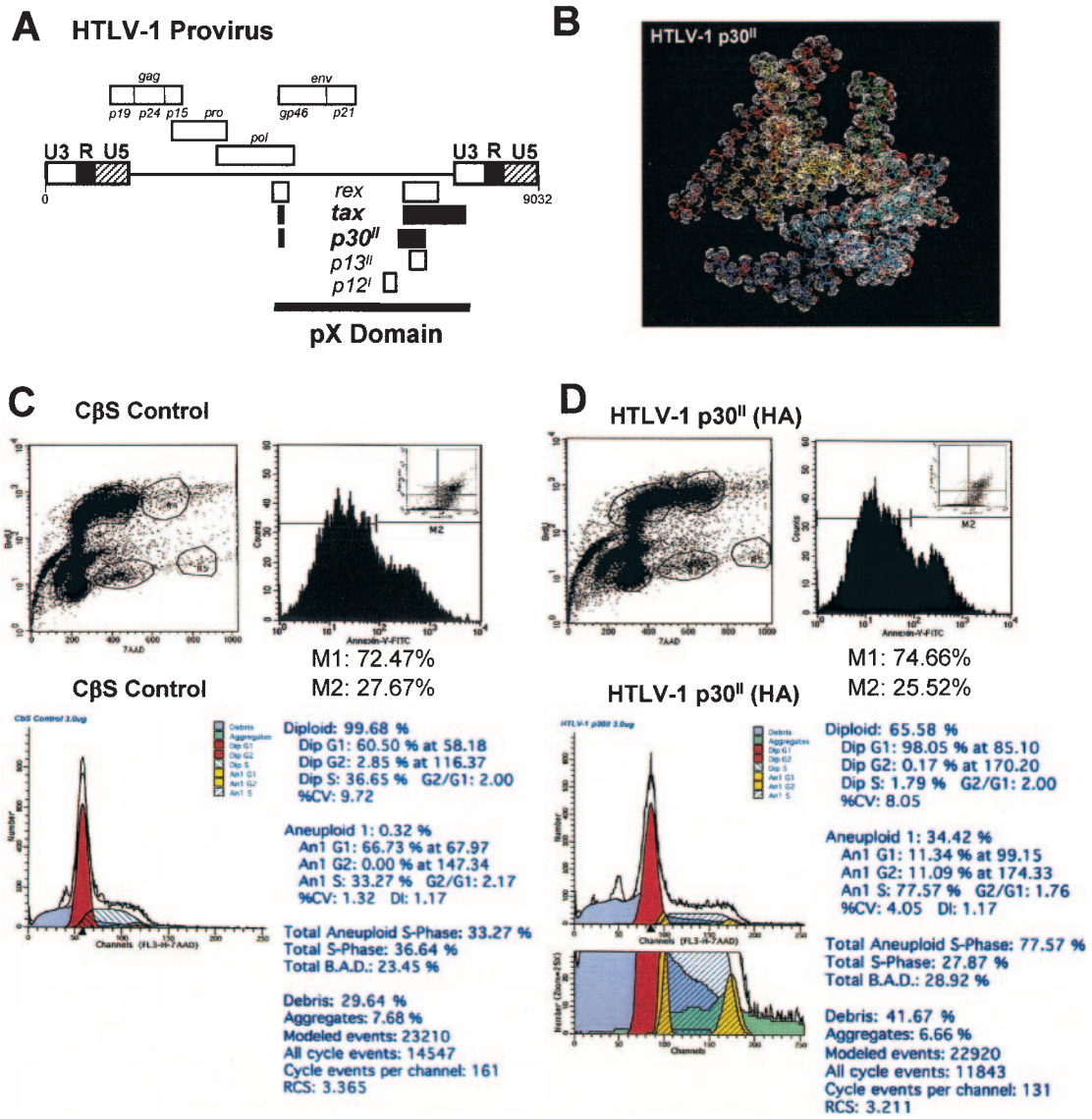

FIG. 1. HTLV-1 p30^{II} increases S-phase cell cycle progression and promotes polyploidy. (A) Diagram of the HTLV-1 proviral genome and its translation products. The pX domain is indicated, and the viral transcription factors Tax and p30^{II} are in boldface type (29). (B) A RasMol structural prediction of the HTLV-1 p30^{II} protein is shown; subdomains (4 alpha-helices; 19 beta-sheets) are represented by different colors and Connelly/Richards (1.2-Å) radii are indicated in white. (C) Molt-4 lymphocytes were transfected with an empty CβS vector control (3.0 μg), and S-phase cells were labeled by BrdU incorporation (*y* axis, upper left). Total DNA content was determined by staining with 7-AAD (*x* axis, upper left). Flow cytometry was performed, and relative percentages of cells in various stages of the cell cycle were quantified using ModFit LT 3.0 (aneuploid analysis) software (lower panels). (D) Molt-4 lymphocytes were transfected with CMV-HTLV-1 p30^{II} (HA) (3.0 μg), percentages of S-phase cells were determined by BrdU-labeling/7-AAD-staining, and cell cycle analyses were performed as described for panel C. Half of each transfected culture was analyzed by staining with annexin V-(FITC)/propidium iodide, and percentages of apoptotic cells were quantified by FACS (panels C and D, upper right). Dip, diploid; An, aneuploid.

fected cells by immunoblotting using a monoclonal anti-HA antibody (CA5; Roche Molecular Biochemicals) (Fig. 3A). Intracellular levels of Myc were not altered by HTLV-1 p30^{II} expression (Fig. 3A, lower panels). HTLV-1 p30^{II} also transcriptionally activates the human cyclin D2 promoter in transfected 293A fibroblasts in a dose-dependent manner (Fig. 3C). To confirm that HTLV-1 p30^{II} promotes Myc-dependent transcription from E-box enhancer elements, we cotransfected 293A fibroblasts and HeLa cells with a synthetic *tk* minimal promoter-luciferase reporter construct (M4-tk-luc) that contains four tandem E-boxes (79). As shown in Fig. 3D, HTLV-1 p30^{II} transactivates E-box enhancer elements within M4-tk-luc, suggesting that p30^{II} promotes S-phase progression through Myc-dependent transcriptional interactions. Interestingly, we observed that p30^{II}, at the lowest concentration used, induced approximately 13-fold transactivation from the synthetic M4-tk-luc promoter, whereas higher concentrations induced lower (5- to 7-fold) levels of transcriptional activation (Fig. 3D). These observations are consistent with findings by Zhang et

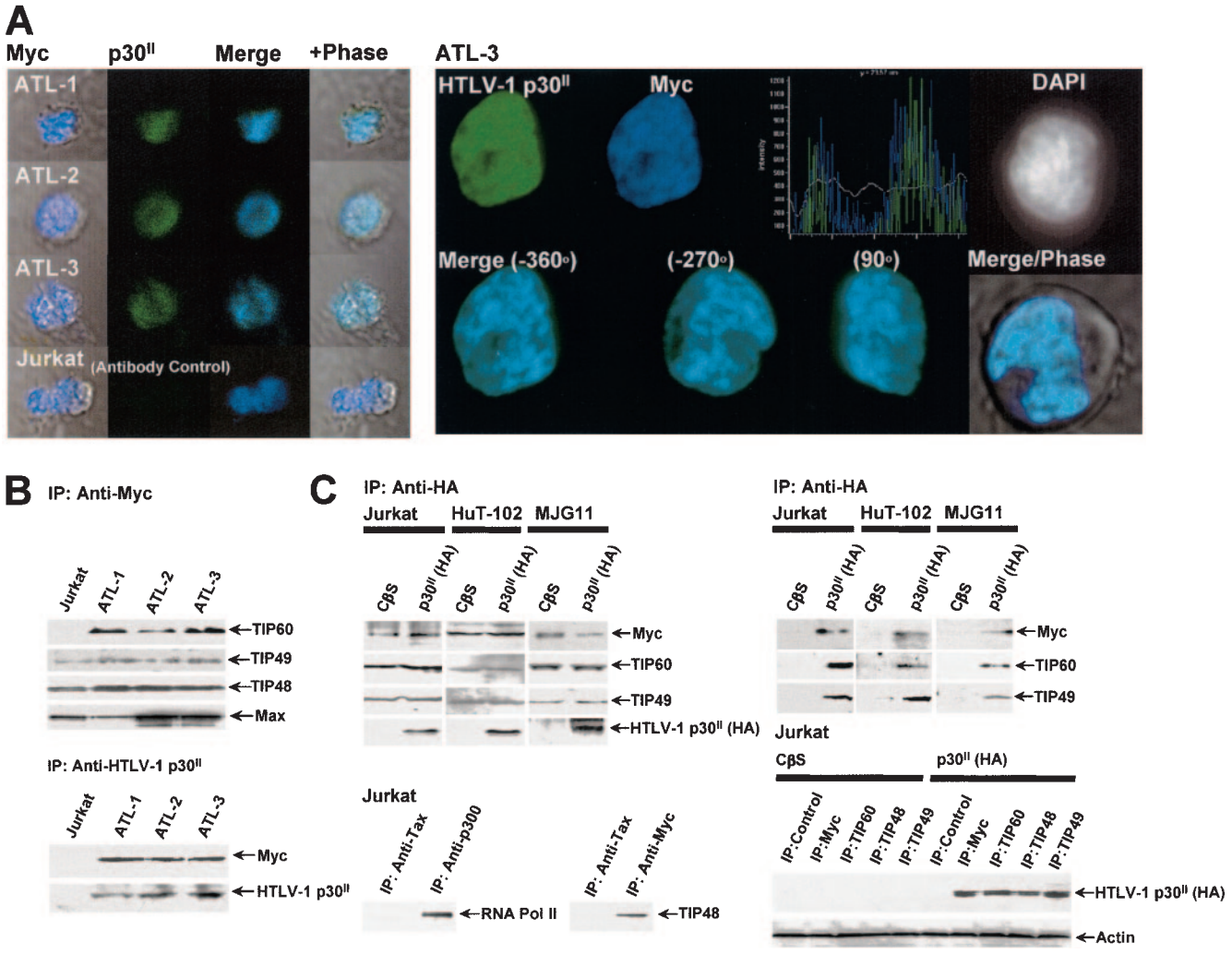

FIG. 2. HTLV-1 p30II interacts with Myc-TIP60 complexes in cultured ATLL patient-derived lymphocytes. (A) Immunofluorescence laser confocal microscopy was performed on HTLV-1-infected ATLL patient-derived T cells (ATL-1, ATL-2, and ATL-3) or Jurkat E6.1 lymphocytes as a negative control, using a rabbit polyclonal anti-HTLV-1 p30II antibody (34) and a monoclonal anti-Myc antibody (Upstate Biotechnology). HTLV-1 p30II was detected using a FITC-conjugated anti-rabbit secondary antibody (green), and Myc was detected using a Cy5-conjugated anti-mouse secondary antibody (blue; Jackson ImmunoResearch Laboratories). A three-dimensional Z-stack composite for ATL-3 is shown on the right. Three rotational views of merged images are shown, demonstrating nuclear colocalization of HTLV-1 p30II (green)/Myc (blue) in all focal planes. Graphical representations of relative fluorescence intensities for HTLV-1 p30II/Myc-specific signals are shown, and DAPI nuclear staining is shown for reference. (B) Coimmunoprecipitations were performed using extracts prepared from HTLV-1-infected ATLL patient-derived lymphocytes and anti-Myc or anti-HTLV-1 p30II antibodies. Interacting proteins were detected by immunoblotting with appropriate primary antibodies. (C) Jurkat E6.1 or HTLV-1-infected HuT-102 and MJ[G11] lymphocytes were transfected with an empty CβS vector control or CMV-HTLV-1 p30II (HA) (5.0 μg), and coimmunoprecipitations were performed using a monoclonal anti-HA tag antibody (CA5; Roche Molecular Biochemicals). HTLV-1 p30II-interacting proteins were detected by immunoblotting. Input levels for immunoprecipitated factors in Jurkat E6.1, HuT-102, and MJ[G11] extracts are provided. HTLV-1 p30II (HA) expression is also shown. RNA polymerase II and TIP48 were immunoprecipitated from Jurkat E6.1 whole-cell extracts using antibodies against known binding partners (anti-p300 and anti-Myc). An anti-HTLV-1 Tax monoclonal antibody (22) was used as a negative control. The HTLV-1 p30II (HA) protein was reimmunoprecipitated from extracts prepared from Jurkat E6.1 lymphocytes and transfected with either a CβS vector control or CMV-HTLV-1 p30II (HA), using antibodies against Myc, TIP60, TIP48, TIP49, or nonspecific rabbit preimmune serum (Control). Input levels for actin are shown for comparison. IP, coimmunoprecipitation.

al. (87) demonstrating that p30II-dependent transactivation from the HTLV-1 promoter (Tax-responsive elements) occurs maximally at low p30II concentrations and diminishes with increased p30II expression (87).

Transcriptional activation by HTLV-1 p30II is dependent upon the TIP60 and TRRAP/p434 coactivators. Frank et al. reported that Myc interacts with the transcriptional coactivator/HAT, TIP60 (16), and Patel et al. have recently shown that c-Myc is a substrate for lysine acetylation by TIP60 and hGCN5 (56). Myc has also previously been demonstrated to interact in chromatin-remodeling complexes with the ATM-related TRRAP/p434 protein (41, 42, 51). Therefore, we tested whether HTLV-1 p30II-mediated transactivation requires TIP60 and TRRAP/p434 functions. HeLa cells were cotrans-

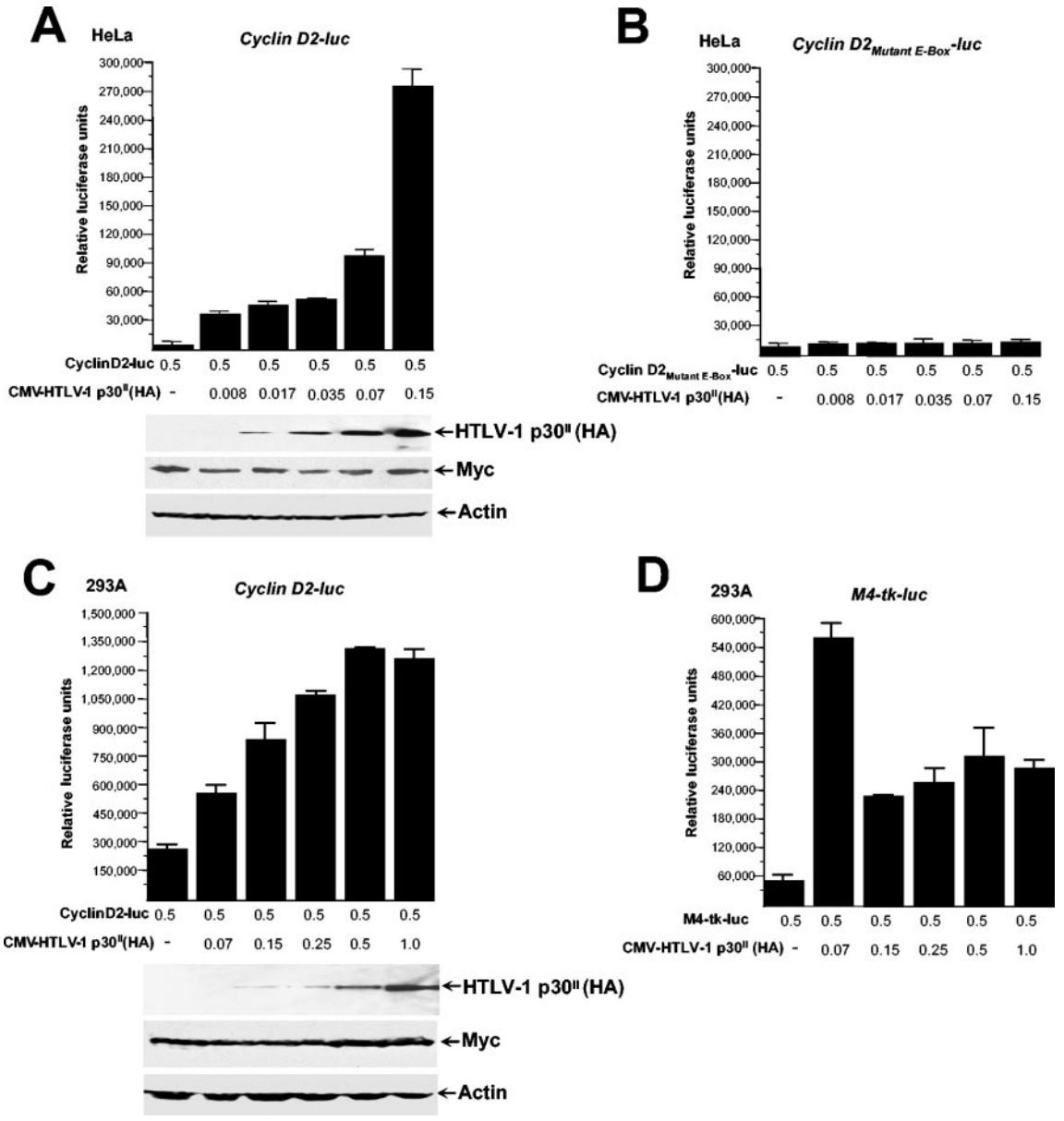

FIG. 3. HTLV-1 $p30^{II}$ transcriptionally activates Myc-responsive elements within the human cyclin D2 promoter. (A) HeLa cells were cotransfected with a human cyclin D2 promoter-luciferase reporter plasmid (0.5 μg) (7) and increasing amounts of CMV-HTLV-1 $p30^{II}$ (HA) (0.008, 0.017, 0.035, 0.07, and 0.15 μg). Cells were lysed by freeze-thawing, and luciferase assays were carried out using equivalent levels of total cellular proteins. The expression of HTLV-1 $p30^{II}$ (HA), Myc, and actin in transfected cells is shown. (B) HeLa cells were cotransfected as described for panel A, with a mutant cyclin D2 promoter-luciferase construct lacking conserved Myc-responsive E-box enhancer elements (0.5 μg) (7) and increasing amounts of CMV-HTLV-1 $p30^{II}$ (HA). (C) 293A fibroblasts were cotransfected as described for panel A, with a human cyclin D2 promoter-luciferase reporter plasmid and increasing amounts of CMV-HTLV-1 $p30^{II}$ (HA) (0.07, 0.15, 0.25, 0.5, 1.0 μg); luciferase assays were performed as described above, using equivalent levels of total cellular proteins. HTLV-1 $p30^{II}$ (HA), Myc, and actin proteins were detected by immunoblotting (lower panels). (D) 293A fibroblasts were cotransfected as described for panel A with a synthetic, E-box-containing minimal *tk* promoter-luciferase reporter construct (M4-tk-luc; 0.5 μg) (79) and increasing amounts of CMV-HTLV-1 $p30^{II}$ (HA) (0.07, 0.15, 0.25, 0.5, and 1.0 μg). All luciferase assays were performed in duplicate or triplicate, and results from representative experiments are shown; error bars representing standard deviations are provided.

fected with a human cyclin D2 promoter-luciferase reporter construct and CMV-HTLV-1 $p30^{II}$ (HA) in the presence of increasing amounts of CMV-TIP60, CMV-$TIP60_{\Delta HAT}$ (a trans-dominant-negative HAT-inactive mutant [25]), or CMV-$TIP60_{L497A}$, a COOH-terminal mutant impaired for interactions with cellular factors, including the androgen receptor (17). Ectopic expression of TIP60 alone did not significantly transactivate the human cyclin D2 promoter; however, TIP60 overexpression enhanced HTLV-1 $p30^{II}$-mediated transactivation in a dose-dependent manner (Fig. 4A). The trans-dominant-negative $TIP60_{\Delta HAT}$ mutant potently inhibited $p30^{II}$-mediated transcriptional activation (Fig. 4A), suggesting that

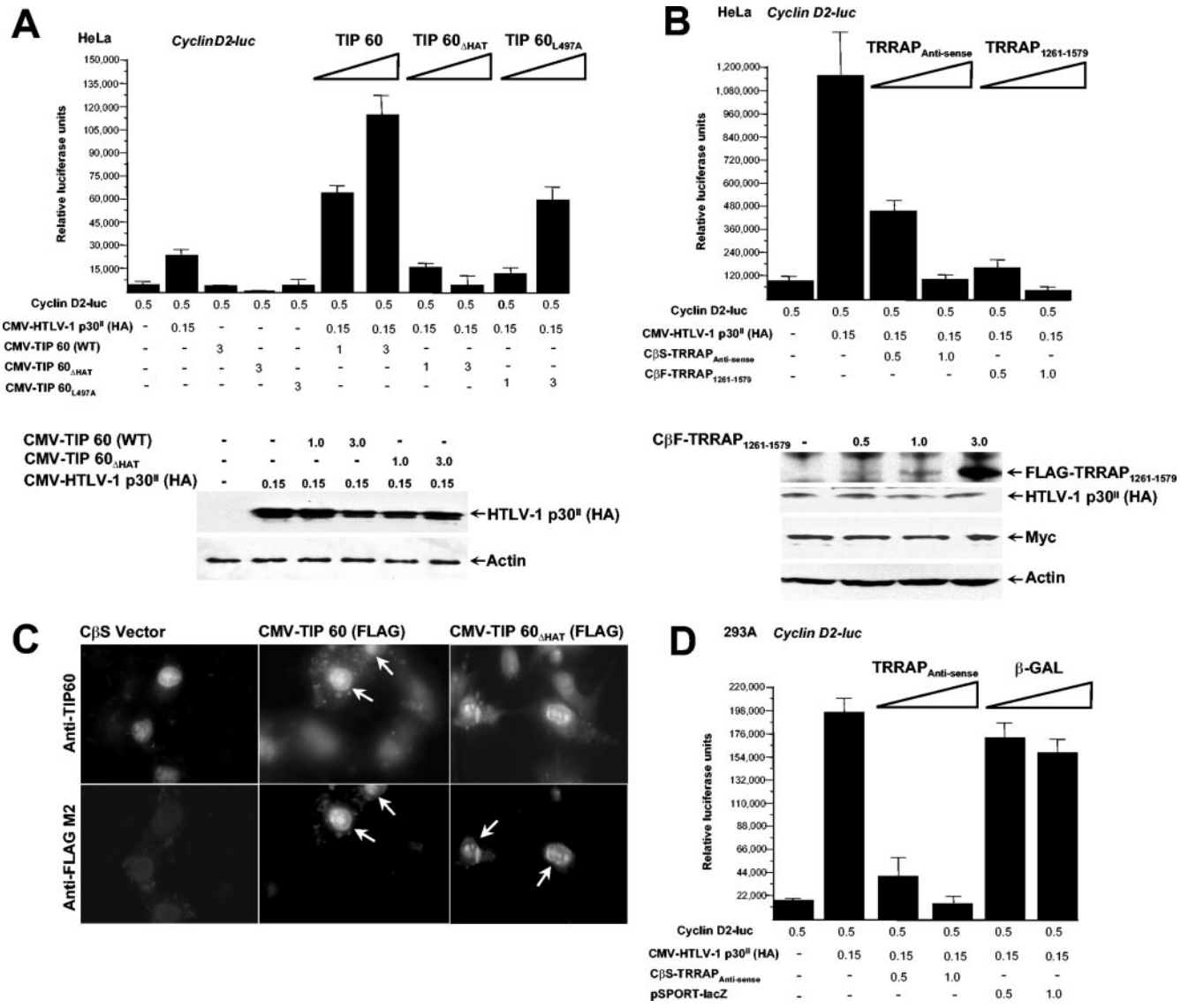

FIG. 4. HTLV-1 p30^{II}-mediated transactivation requires the transcriptional coactivators TIP60 and TRRAP. (A) HeLa cells were cotransfected with a human cyclin D2 promoter-luciferase reporter plasmid (0.5 μg) and CMV-HTLV-1 p30^{II} (HA) (0.15 μg) in the presence of increasing amounts of CMV-wild-type TIP60, CMV-TIP60$_{\Delta HAT}$, or CMV-TIP60$_{L497A}$ (1.0 and 3.0 μg) (17, 25). Expression of HTLV-1 p30^{II} (HA) and actin was detected by immunoblotting (lower panels). (B) HeLa cells were cotransfected as described for panel A with a human cyclin D2 promoter-luciferase plasmid and CMV-HTLV-1 p30^{II} (HA) in the presence of increasing amounts of CβS-TRRAP$_{antisense}$ or CβF-TRRAP$_{1261-1579}$ (0.5 and 1.0 μg) (41). Expression of the trans-dominant-negative TRRAP$_{1261-1579}$-(FLAG) mutant, HTLV-1 p30^{II} (HA), Myc, and actin proteins was detected by immunoblotting using an anti-FLAG M2 monoclonal antibody (Sigma Chemical Corp.), anti-HA (CA5) or anti-Myc monoclonal antibodies, or anti-actin goat polyclonal antibody. All luciferase assays were performed in duplicate or triplicate, and results from representative experiments are shown; error bars representing standard deviations are provided. (C) Overexpression of the (FLAG)-TIP60 (wild-type) and (FLAG)-TIP60$_{\Delta HAT}$ proteins (25) relative to endogenous TIP60 was visualized by immunofluorescence microscopy using a rabbit polyclonal anti-TIP60 antibody (top panels) and an anti-FLAG M2 monoclonal antibody (bottom panels). The CβS empty vector was transfected as a negative control. (D) To confirm the specificity of transcriptional inhibition by TRRAP$_{antisense}$ RNA, 293A fibroblasts were cotransfected with human cyclin D2 promoter-luciferase and CMV-HTLV-1 p30^{II} (HA) plasmids in the presence of either increasing amounts (0.5 and 1.0 μg) of CβS-TRRAP$_{antisense}$ (41) or of pSPORT-*lacZ*, which expresses β-galactosidase mRNA. Relative luciferase activities were determined from duplicate assays using approximately equivalent levels of total cellular proteins.

HTLV-1 p30^{II} transactivation requires TIP60-associated HAT activity (25). The TIP60$_{L497A}$ mutant also weakly enhanced p30^{II}-mediated transactivation (Fig. 4A). Overexpression of wild-type TIP60 or the trans-dominant-negative TIP60$_{\Delta HAT}$ mutant did not alter expression of the HTLV-1 p30^{II} (HA) protein in transfected HeLa cells (Fig. 4A, lower panels). Inhibition of TRRAP/p434, as a result of coexpressing either TRRAP$_{antisense}$ RNA or a trans-dominant-negative TRRAP mutant, TRRAP$_{1261-1579}$ (FLAG-epitope-tagged [41]), prevented HTLV-1 p30^{II}-mediated transcriptional activation from the human cyclin D2 promoter (Fig. 4B). The trans-dominant-negative, FLAG-tagged TRRAP$_{1261-1579}$ protein did not alter

the expression of HTLV-1 $p30^{II}$ (HA) (Fig. 4B, lower panels). We then performed immunofluorescence microscopy, using a monoclonal anti-FLAG M2 antibody (Sigma Chemical Corp.) and a rabbit polyclonal anti-TIP60 antibody (Upstate Biotechnology), to visualize expression of the FLAG-tagged wild-type TIP60 or $TIP60_{\Delta HAT}$ proteins relative to endogenous TIP60 (25). Results shown in Fig. 4C demonstrate that the FLAG-tagged TIP60 proteins were drastically overexpressed relative to endogenous TIP60 in transfected cells. To demonstrate the specificity of transcriptional inhibition due to $TRRAP_{antisense}$ RNA in panel B, we repeated these experiments using a pSPORT-*lacZ* control plasmid which expresses β-galactosidase mRNA. Results shown in Fig. 4D demonstrate that increased β-galactosidase mRNA expression did not influence HTLV-1 $p30^{II}$-dependent transactivation from the cyclin D2 promoter, whereas $TRRAP_{antisense}$ inhibited $p30^{II}$ transcriptional activation in a dose-dependent manner. These data collectively indicate that HTLV-1 $p30^{II}$ synergizes with the TIP60 HAT to transactivate Myc-responsive E-box elements within the human cyclin D2 promoter, requiring the transcriptional coactivator TRRAP/p434 (7, 25, 41, 79).

HTLV-1 $p30^{II}$ stabilizes Myc/TIP60 chromatin-remodeling transcription complexes in HTLV-1-infected lymphocytes. As we have shown that HTLV-1 $p30^{II}$ transcriptionally activates the conserved Myc-responsive E-box enhancer elements within the human cyclin D2 promoter (Fig. 3A and C) (7), we sought to determine whether $p30^{II}$ is present in Myc-containing chromatin-remodeling complexes using the ChIP procedure as described by Vervoorts et al. (79). Formaldehyde cross-linked genomic DNA complexes in uninfected Molt-4 lymphocytes or HTLV-1-infected MJ[G11] and HuT-102 lymphocytes were fragmented by sonication, and oligonucleosomal-protein complexes were precipitated using antibodies against candidate Myc-binding factors. Cross-links were reversed, and specific oligonucleotide DNA primer pairs were used in PCRs to amplify immunoprecipitated DNA regions spanning conserved E-box elements (PRM) or an untranslated sequence (UTR) as negative control (79). Results in Fig. 5A (top panels) demonstrate that HTLV-1 $p30^{II}$ was detected only bound to E-box enhancer elements in HTLV-1-infected lymphocytes. Myc, TRRAP, TIP49 (RUVBL1), TIP48 (RUVBL2), and the acetyltransferase hGCN5 (42) were present in chromatin-remodeling complexes in uninfected Molt-4 cells and in HTLV-1-infected MJ[G11] and HuT-102 lymphocytes (Fig. 5A, top panels). Surprisingly, TIP60 was detected only in Myc-containing transcription complexes that contained $p30^{II}$ in HTLV-1-infected T cells (Fig. 5A, top panels), consistent with coimmunoprecipitation results and observed effects of ectopic TIP60 in transactivation assays (see Fig. 2B and 4A). The diminished recruitment of TIP49 to Myc-containing transcription complexes on the cyclin D2 promoter in HTLV-1-infected MJ[G11] cells was not attributable to apparent differences in $p30^{II}$/Myc/TIP60 interactions (Fig. 5A). Histone H3 acetylation surrounding the E-box enhancer elements within the human cyclin D2 promoter, consistent with transcriptional activation, was detected in all cell types with the exception of H3, which appeared to be differentially acetylated on Lys-9 and Lys-14 residues in HTLV-1-infected MJ[G11] and HuT-102 cells, respectively (Fig. 5A, lower panels). Differences in histone H3 acetylation, however, did not correlate with the stabilization of $p30^{II}$/Myc/TIP60 transcriptional interactions in HTLV-1-infected T-cell lines.

To identify residues within HTLV-1 $p30^{II}$ that interact with Myc/TIP60 complexes in vivo, we generated a panel of pGEX 4T.1-glutathione *S*-transferase (GST)-HTLV-1 $p30^{II}$ constructs, expressing full-length GST-HTLV-1 $p30^{II}$ or various truncation mutants, GST-$p30^{II}$ (residues 1 to 98), GST-$p30^{II}$ (residues 99 to 154), GST-$p30^{II}$ (residues 155 to 241) spanning the entire coding region of HTLV-1 $p30^{II}$ (Fig. 5B, see diagram). These proteins were expressed in *Escherichia coli* BL21 bacteria, and purified recombinant GST-HTLV-1 $p30^{II}$ fusion proteins were used in GST pull-down experiments as described by Harrod et al. (23). GST proteins were incubated with HeLa nuclear extracts at 4°C overnight, and complexes were precipitated with glutathione-Sepharose 4B (Amersham-Pharmacia Biotech). The matrices were washed, and bound factors were eluted using 10 mM reduced glutathione buffer. Input levels of purified recombinant GST or GST-HTLV-1 $p30^{II}$ proteins, Myc, and TIP60 are shown in Fig. 5B. Results shown in Fig. 5B (right panels) demonstrate that full-length GST-HTLV-1 $p30^{II}$ interacts with both Myc and TIP60 in HeLa nuclear extracts. Deletion of amino acid residues from either the NH_2 terminus or COOH terminus of $p30^{II}$ disrupts Myc binding; however, the TIP60-interacting region of HTLV-1 $p30^{II}$ was mapped to residues between positions 99 and 154 (Fig. 5B). Our future efforts will biochemically characterize specific amino acid contacts responsible for the stabilization of HTLV-1 $p30^{II}$/Myc/TIP60 transcriptional interactions.

We next examined recruitment of HTLV-1 $p30^{II}$/Myc/TIP60 chromatin remodeling complexes to conserved, Myc-responsive E-box enhancer elements within the cyclin D2 promoter in cultured HTLV-1-infected ATLL patient lymphocytes (ATL-1). Chromatin-immunoprecipitations were performed using antibodies that recognize endogenous HTLV-1 $p30^{II}$ (34), Myc, and known Myc-interacting factors as described previously. Polymerase chain-reaction amplification of ChIP products was performed using the PRM and UTR oligonucleotide DNA primer pairs (79). Results shown in Fig. 5C demonstrate that $p30^{II}$ is present in Myc/TIP60 transcription complexes assembled on E-box enhancer elements within the cyclin D2 promoter in HTLV-1 ATLL patient lymphocytes. The transcriptional coactivators, TRRAP/p434, TIP48, TIP49, and hGCN5 were also detected in $p30^{II}$/Myc/TIP60/cyclin D2 promoter complexes (Fig. 5C).

HTLV-1 $p30^{II}$-GFP stabilizes Myc/TIP60 interactions and transactivates the cyclin D2 promoter in a TIP60 HAT-dependent manner. We next investigated whether HTLV-1 $p30^{II}$ interacts similarly in Myc/TIP60 transcription complexes in 293A fibroblasts. Nicot et al. (48) have demonstrated that an HTLV-1 $p30^{II}$-green fluorescent protein (GFP) is functionally identical to HTLV-1 $p30^{II}$ (HA) (48). We therefore cotransfected 293A cells with CMV-HTLV-1 $p30^{II}$-GFP (kindly provided by G. Franchini, NCI, NIH [48]) or a pcDNA3.1-GFP vector control and performed ChIP analyses. Nucleoprotein complexes were cross-linked by treatment with formaldehyde, and oligonucleosomal fragments were generated by brief sonication of extracted genomic DNA. Chromatin immunoprecipitations were performed as described above, and ChIP products were amplified by PCR using the PRM and UTR oligonucleotide DNA primer pairs (79). Similar expression of

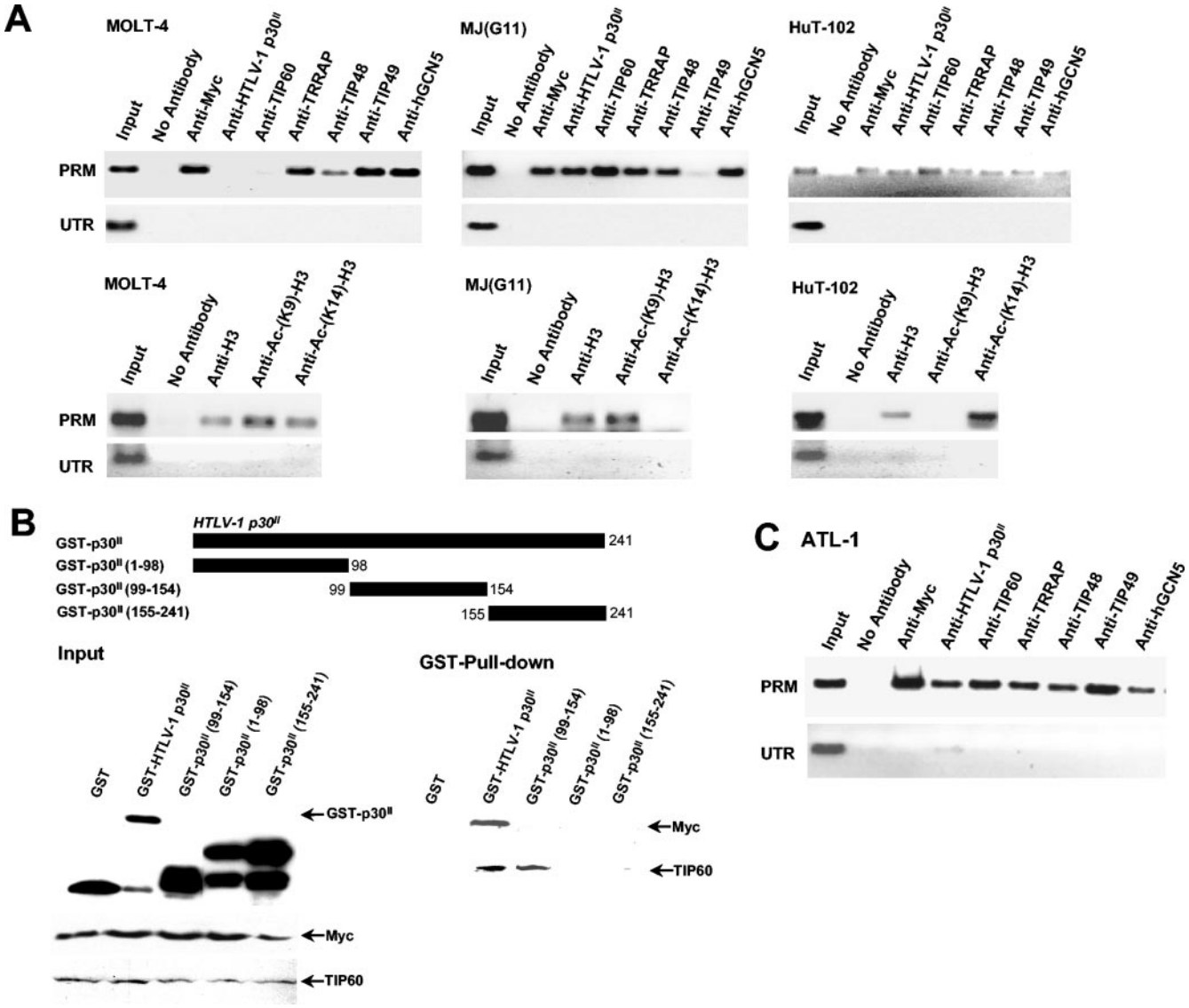

FIG. 5. HTLV-1 $p30^{II}$ is present in Myc-TIP60-containing chromatin-remodeling complexes in HTLV-1-infected lymphocytes. (A) Chromatin immunoprecipitation assays were performed with uninfected Molt-4 lymphocytes or HTLV-1-infected MJ[G11] and HuT-102 lymphocytes using antibodies that recognize various Myc-interacting factors (TIP60, TRRAP, TIP48, TIP49, and hGCN5; top panels) or acetylated forms of histone H3 (acetyl-K9 and acetyl-K14; lower panels). The PRM primer pair anneals to sequences flanking the conserved E-box elements within the human cyclin D2 promoter, and the UTR negative control primers anneal within an untranslated region (79). (B) Purified recombinant GST-HTLV-1 $p30^{II}$ or GST-$p30^{II}$ (1 to 98), GST-$p30^{II}$ (99 to 154), and GST-$p30^{II}$ (155 to 241) truncated mutant proteins were incubated with HeLa nuclear extracts, and GST pull-down assays were performed as described previously (23) using glutathione-Sepharose 4B (Amersham-Pharmacia Biotech). A diagram of GST-HTLV-1 $p30^{II}$ fusion proteins and relative input levels of GST-HTLV-1 $p30^{II}$ and GST-$p30^{II}$ truncation mutants, Myc, and TIP60 proteins is shown. Results from GST pull-down experiments are provided in the panels on the right. (C) ChIP analyses of HTLV-1 $p30^{II}$-Myc/TIP60 transcription complexes recruited to Myc-responsive E-box elements within the genomic cyclin D2 promoter in cultured lymphocytes from an HTLV-1-infected ATLL patient (ATL-1). Chromatin immunoprecipitations were performed as for panel A, and PCR analyses of ChIP products were carried out using PRM and UTR oligonucleotide primer pairs (79).

HTLV-1 $p30^{II}$-GFP and GFP proteins was visualized with transfected 293A fibroblasts by fluorescence microscopy (Fig. 6A and B). The HTLV-1 $p30^{II}$-GFP protein was immunoprecipitated and bound to Myc-containing transcription complexes on conserved E-box elements within the cyclin D2 promoter in transfected 293A fibroblasts, using an anti-GFP antibody (Fig. 6A). No ChIP product was detected for the anti-GFP immunoprecipitation in 293A cells transfected with the pcDNA3.1-GFP control (Fig. 6B). While the transcriptional coactivators TRRAP/p434, TIP48, TIP49, and hGCN5 were present in Myc-containing complexes in both HTLV-1 $p30^{II}$-GFP and GFP-expressing cells, the TIP60 HAT was detected predominantly in HTLV-1 $p30^{II}$-GFP/Myc/TIP60 complexes (compare Fig. 6A and B). However, TIP60 was weakly present in Myc-containing ChIP complexes in GFP-expressing cells, consistent with the demonstration of pre-existing Myc-TIP60 interactions by Frank et al. (16) and Patel et al. (56) (Fig. 6B).

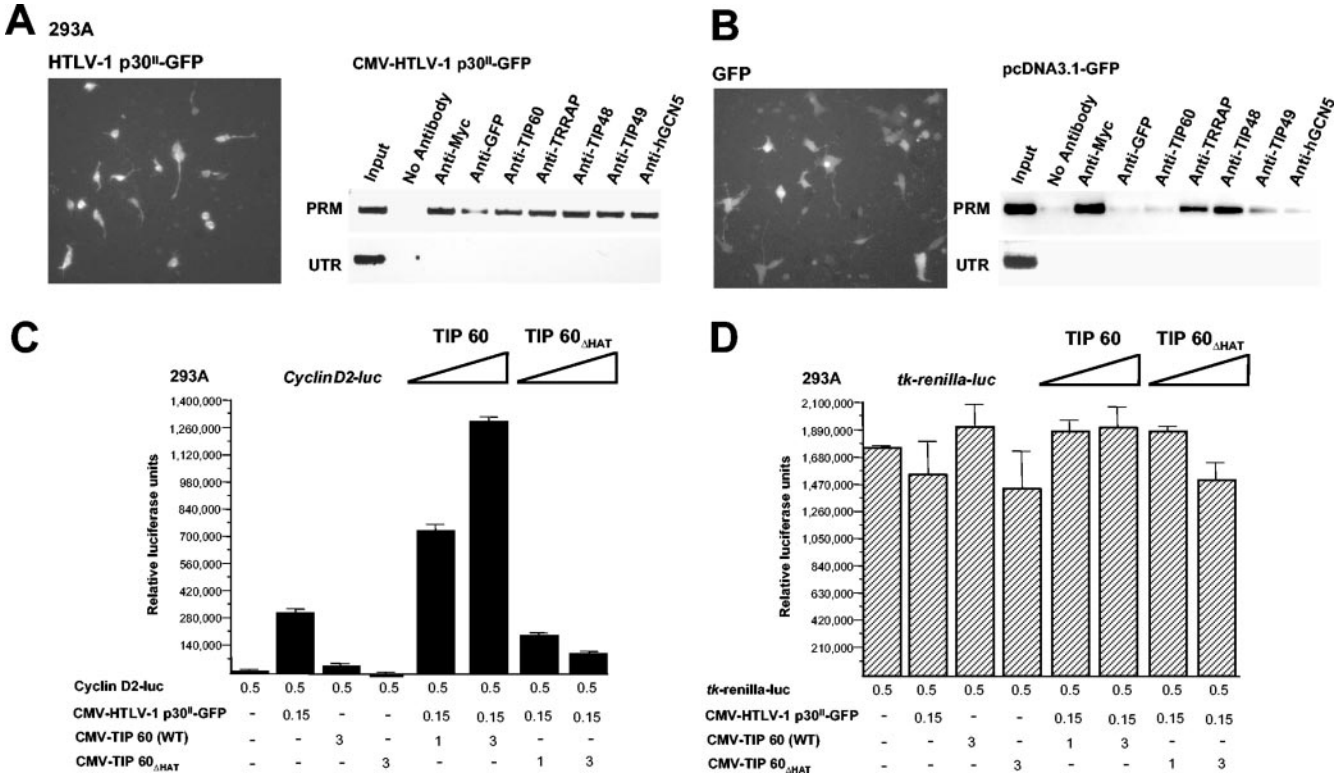

FIG. 6. HTLV-1 p30^{II}-GFP interacts in Myc/TIP60 transcription complexes and transcriptionally activates the human cyclin D2 promoter. (A) 293A fibroblasts were transfected with HTLV-1 p30^{II}-GFP (48), and ChIP analyses were performed using various antibodies against specific Myc-interacting proteins. Expression of HTLV-1 p30^{II}-GFP in transfected cells was visualized by fluorescence microscopy (left panel). Polymerase chain reaction amplification of ChIP products was carried out using the PRM and UTR oligonucleotide primer pairs as described previously (79). (B) 293A fibroblasts were transfected with a pcDNA3.1-GFP control, and ChIP analyses were performed as described for panel A. Expression of GFP was detected in transfected 293A cells by fluorescence microscopy. (C) 293A fibroblasts were cotransfected with a human cyclin D2 promoter-luciferase reporter construct (0.5 μg), *tk* promoter-*Renilla* luciferase reporter construct (0.5 μg), CMV-HTLV-1 HTLV-1 p30^{II}-GFP (0.15 μg), and increasing amounts (1.0 and 3.0 μg) of CMV-TIP60 (wild type) or CMV-TIP60$_{\Delta HAT}$ (25). Dual luciferase assays were performed to measure transcriptional activation. (D) Relative *Renilla* luciferase activities for each sample are shown. Error bars representative of standard deviations from duplicate experiments are provided. WT, wild type.

To determine whether the HTLV-1 p30^{II}-GFP protein also transcriptionally activates the human cyclin D2 promoter in a TIP60-dependent manner, we cotransfected 293A fibroblasts with a *tk* promoter-*Renilla* luciferase plasmid, a human cyclin D2 promoter-luciferase reporter plasmid, and CMV-HTLV-1 p30^{II}-GFP in the presence of increasing amounts of either CMV-TIP60 (wild-type) or CMV-TIP60$_{\Delta HAT}$, which expresses a trans-dominant-negative TIP60 mutant (7, 25, 48). Results shown in Fig. 6C demonstrate that HTLV-1 p30^{II}-GFP transcriptionally activates the human cyclin D2 promoter approximately 14-fold in transfected 293A fibroblasts compared to an empty pcDNA3.1-GFP control. Overexpression of wild-type TIP60, in the presence of HTLV-1 p30^{II}-GFP, significantly increased p30^{II}-GFP-dependent transcriptional activity in a dose-dependent manner (Fig. 6C). Coexpression of the trans-dominant-negative TIP60$_{\Delta HAT}$ mutant (25) repressed p30^{II}-GFP-dependent transactivation from the human cyclin D2 promoter (Fig. 6C), consistent with the results shown in Fig. 4A and with an essential role for the TIP60 HAT in HTLV-1 p30^{II} transcriptional activation. Relative *Renilla* luciferase activities for each sample are shown in Fig. 6D for comparisons of similar transfection efficiencies.

HTLV-1 p30^{II} transcriptionally activates numerous cellular genes in a TIP60-dependent or TIP60-independent manner. To comprehensively identify cellular gene sequences whose expressions are altered by HTLV-1 p30^{II}-TIP60 transcriptional interactions, we cotransfected 293A fibroblasts with a CβS empty vector control, CMV-HTLV-1 p30^{II} (HA), or CMV-HTLV-1 p30^{II} (HA) and TIP60$_{\Delta HAT}$, which expresses a trans-dominant-negative mutant that interferes with endogenous TIP60 functions (25). Total cellular RNAs were extracted, and microarray gene expression analyses were performed using Affymetrix Human U133Plus 2.0 full-genomic chips. Transcriptional activation of cellular target genes is expressed as activation (*n*-fold) relative to the empty CβS vector control, and the lower limit for transactivation was set at 2.5-fold. Figure 7A shows a graphical representation of cellular target genes transcriptionally activated by HTLV-1 p30^{II} (HA) (red lines). TIP60-dependent gene sequences were identified based upon their transcriptional repression in the presence of the TIP60$_{\Delta HAT}$ mutant (25) and are indicated by green lines (Fig. 7A). In general, the fold transactivation by HTLV-1 p30^{II} (HA) ranged between 2.5-fold to 393-fold for specific target genes (Fig. 7A). Michael et al. (44) have demonstrated that

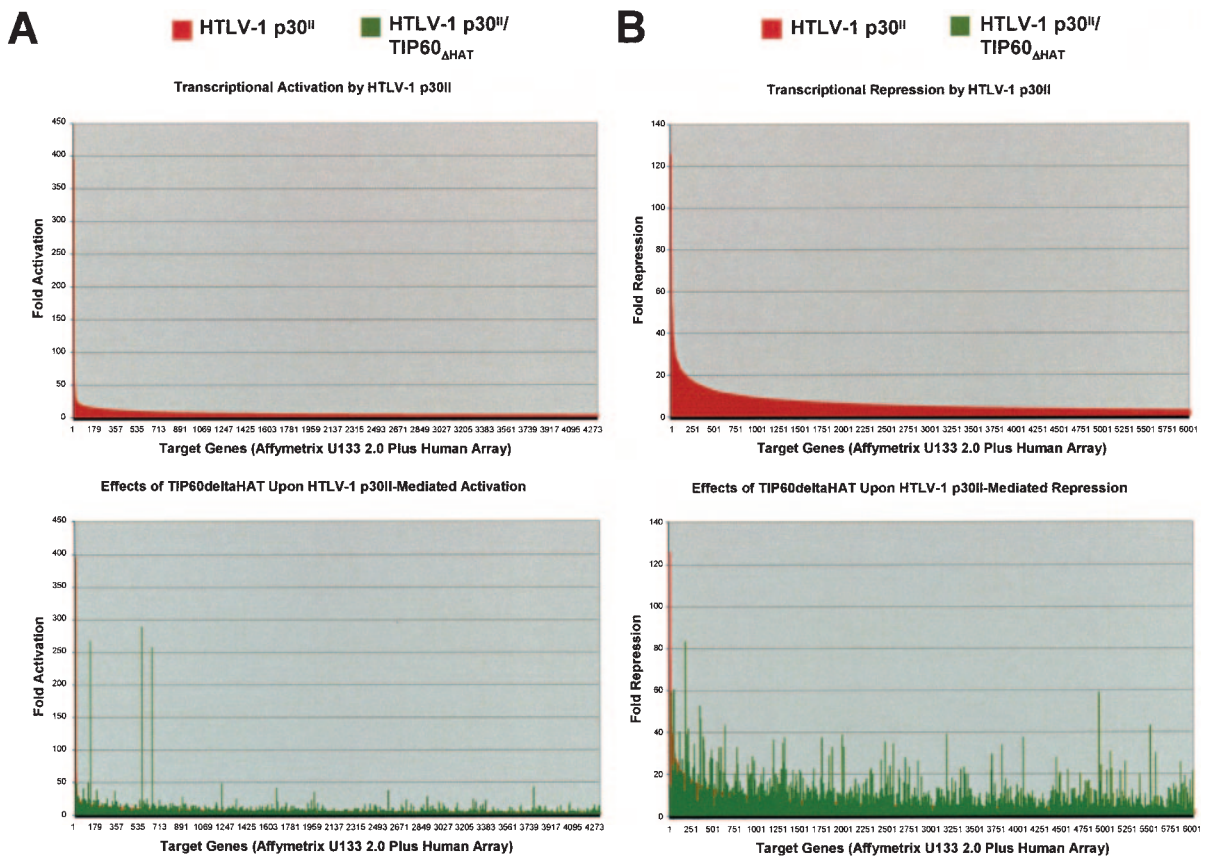

C ***Target sequences transcriptionally-activated by HTLV-1 p30II(HA) in a TIP60-dependent or TIP60-independent manner*** *(Fold Activation)*

HTLV-1 p30II	*HTLV-1 p30II/ TIP60ΔHAT*	*Gene or Sequence Identity*
		TITLE=zinc finger protein 236 /DEF=Homo sapiens
393.8725	396.7248	cDNA FLJ20840 fis, clone ADKA02336.
69.33333	2.666667	Homo sapiens, clone IMAGE:4813412, mRNA
65.5	7	Hs.42369 /UG_TITLE=ESTs
56	46.4	UG=Hs.66114 /UG_TITLE=ESTs
		CPX chromosome region, candidate 1 /DEF=Homo
52.75	1	sapiens cDNA FLJ25780 fis, clone TST06618.
49.09091	0.909091	Hs.131856 /UG_TITLE=ESTs
48	43	Hs.23196 /UG_TITLE=ESTs
45.4	43.06667	Hs.116301 /UG_TITLE=ESTs
40.44444	18.22222	Hs.200286 /UG_TITLE=ESTs
40.16667	22	Homo sapiens, clone IMAGE:4812574, mRNA.
34.625	49.375	Homo sapiens, clone IMAGE:5172609, mRNA.
34.44444	3.444444	Hs.122442 /UG_TITLE=ESTs
		Homo sapiens cystic fibrosis transmembrane conductance regulator isoform 36 (CFTR) mRNA,
31.85714	3.857143	partial cds.
		Homo sapiens myeloid cell nuclear differentiation
31.1875	1	antigen (MNDA), mRNA
31	2.75	Hs.145611 /UG_TITLE=ESTs
30.88889	3.555556	Hs.120414 /UG_TITLE=ESTs
28.06667	10.66667	Hs.125291 /UG_TITLE=ESTs
27.72222	1.722222	H.sapiens mRNA HTPCRX06 for olfactory receptor.
27.625	28	Homo sapiens, clone IMAGE:5223057, mRNA.
26.65217	7.73913	TESTI2017113.
		protocadherin 15 /DEF=Homo sapiens mRNA; cDNA
26.1875	1.5625	DKFZp667A1711 (from clone DKFZp667A1711).
		Hs.279616 /UG_TITLE=ESTs, Highly similar to
25.5	1.333333	KIAA1387 protein (H.sapiens)
		Homo sapiens full length insert cDNA clone
25.16667	11.55556	YW25E05
24.83333	29.83333	Hs.208486 /UG_TITLE=ESTs
		Homo sapiens mRNA; cDNA DKFZp313L0839 (from
24.7619	11.90476	clone DKFZp313L0839).
		Homo sapiens synaptonemal complex protein 1 (SYCP1), mRNA. /PROD=synaptonemal complex
24.71429	14.92857	protein 1 /FL=gb:NM_003176.1 gb:D67
		Homo sapiens cDNA FLJ14020 fis, clone
24.64286	2.785714	HEMBA1002508.
24.09091	27.18182	Homo sapiens, clone IMAGE:5269594, mRNA.
		Hs.99578 /UG_TITLE=ESTs, Highly similar to PTPD_HUMAN PROTEIN-TYROSINE
23.73333	1.933333	PHOSPHATASE DELTA PRECURSOR (H.sapiens)
		H.sapiens mRNA for gonadotropin-releasing hormone receptor, splice variant. /PROD=gonadotropin-
23.58065	22.03226	releasing hormone receptor
		Homo sapiens cDNA FLJ12548 fis, clone NT2RM4000657, weakly similar to 1-
23.3913	4.913043	PHOSPHATIDYLINOSITO

HTLV-1 p30^{II}	HTLV-1 p30^{II}/TIP60$_{\Delta HAT}$	Gene or Sequence Identity
23	2.833333	Homo sapiens cDNA FLJ37910 fis, clone CTONG1000040.
22.65	17.15	Homo sapiens mRNA for pH-sensing regulatory factor of peptide transporter, complete cds.
22.35714	2	Homo sapiens, clone IMAGE:4398590, mRNA.
22.125	0.625	Homo sapiens cDNA: FLJ20870 fis, clone ADKA02524.
21.83333	13.58333	Homo sapiens cDNA FLJ11096 fis, clone PLACE1005480.
21.8	7.1	Hs.60556 /UG_TITLE=ESTs
21.47059	1.058824	Homo sapiens, clone IMAGE:5742085, mRNA.
21.4	1.2	Hs.130544 /UG_TITLE=ESTs
21	7.208333	Hs.222222 /UG_TITLE=ESTs
20.85714	7.214286	Homo sapiens osteoglycin (osteoinductive factor, mimecan) (OGN), mRNA
20.73913	17.82609	Hs.222120 /UG_TITLE=ESTs
20.71429	19.78571	Homo sapiens cDNA FLJ25595 fis, clone JTH13269.
20.7	4.3	Homo sapiens cDNA FLJ13003 fis, clone NT2RP3000418.
20.42857	7.035714	Human DNA sequence from clone 733D15 on chromosome Xp11.3. Contains a Zinc-finger (pseudo?) gene and G
20.42857	6.714286	Hs.132649 /UG_TITLE=ESTs
20.28235	10.15294	Homo sapiens cDNA FLJ11475 fis, clone HEMBA1001734, moderately similar to CADHERIN-11 PRECURSOR
20.25	4.75	Homo sapiens epiregulin (EREG), mRNA
20.2381	15.52381	Homo sapiens cDNA FLJ39700 fis, clone SMINT2011588, weakly similar to Kruppe
20.04545	9.136364	Homo sapiens mRNA; cDNA DKFZp434P2450 (from clone DKFZp434P2450).
19.95238	1	paraneoplastic encephalomyelitis antigen {5 region, alternatively spliced} (human, lung cancer cell line, mRNA Partial, 10
19.78261	15.65217	Homo sapiens aldehyde oxidase 1 (AOX1), mRNA
19.77778	13.77778	Hs.293582 /UG_TITLE=ESTs
19.75	6.833333	Homo sapiens cDNA: FLJ21221 fis, clone COL00570.
19.71795	15.89744	Homo sapiens cDNA FLJ40624 fis, clone THYMU2013981.
19.69565	23.95652	colony stimulating factor 2 receptor, beta, low-affinity (granulocyte-macrophage)
19.6	12.46667	Human deleted in azoospermia protein (DAZ) mRNA, complete cds
19.57143	19.85714	glutamate receptor, ionotropic, kainate 2 /DEF=Homo sapiens mRNA for GluR6 kainate receptor (GRIK2 gene), isoform-b
19.55556	2.111111	hypothetical protein LOC285419 /DEF=Homo sapiens, clone IMAGE:4839001, mRNA
19.52941	1.235294	Homo sapiens sperm associated antigen 11 (SPAG11), transcript variant B, mRNA.
19.25926	9.185185	Homo sapiens mRNA; cDNA DKFZp434L1717 (from clone DKFZp434L1717); complete cds
19.24138	20.31034	Homo sapiens cDNA FLJ35054 fis, clone OCBBF2018380.
19.16667	14.11111	Hs.36683 /UG_TITLE=ESTs
19.07143	8	Hs.106645 /UG_TITLE=ESTs
18.93333	37.53333	Homo sapiens cDNA FLJ11602 fis, clone HEMBA1003908
18.90476	15.38095	Homo sapiens, clone IMAGE:5164933, mRNA
18.71429	40.71429	Hs.176420 /UG_TITLE=ESTs
18.7037	2.222222	Homo sapiens, Similar to BCL2-associated athanogene, clone IMAGE:4310445, mRNA
18.66667	20.06667	DNA segment on chromosome X (unique) 9928 expressed sequence
18.5	5.958333	Homo sapiens PIAS-NY protein mRNA, complete cds
18.47368	4.368421	Homo sapiens full length insert cDNA clone YI41H11
18.46154	4.615385	Homo sapiens pre-TNK cell associated protein (1D12A), mRNA
18.45455	17.24242	Homo sapiens mRNA differentially expressed in malignant melanoma, clone MM K2
18.23529	3.529412	Homo sapiens cDNA FLJ32062 fis, clone OCBBF1000042.
18.14286	6	Hs.204562 /UG_TITLE=ESTs
18.03226	7.451613	Hs.269931 /UG_TITLE=ESTs
18	13.58333	Homo sapiens, clone IMAGE:4393885, mRNA, partial cds
17.76471	24.88235	Hs.23187 /UG_TITLE=ESTs
17.71429	23.07143	Hs.42993 /UG_TITLE=ESTs
17.625	1.5	Homo sapiens glypican 5 (GPC5), mRNA
17.6129	12.12903	Homo sapiens mRNA; cDNA DKFZp686C1636 (from clone DKFZp686C1636)
17.5	21.53125	Hs.213386 /UG_TITLE=ESTs
17.48276	2	Hs.99200 /UG_TITLE=ESTs
17.47826	2.913043	Hs.17388 /UG_TITLE=ESTs
17.47368	6.710526	MCF.2 cell line derived transforming sequence-like /DEF=Homo sapiens, clone IMAGE:5185971, mRNA
17.40541	3.486486	Hs.6656 /UG_TITLE=ESTs
17.36842	15.73684	Hs.22249 /UG_TITLE=ESTs
17.31169	16.42857	Hs.20103 /UG_TITLE=ESTs
17.09091	17.09091	Human (clone CTG-A4) mRNA sequence
17.09091	22.36364	Homo sapiens cDNA FLJ36285 fis, clone THYMU2003470.
17	16.44444	Homo sapiens SAM domain, SH3 domain and nuclear localisation signals, 1 (SAMSN1), mRNA. /PROD=SAM domain, SH3 domain and nuclear
16.83333	17.69444	Homo sapiens, clone MGC:34025 IMAGE:4828588, mRNA, complete cds. /PROD=Unknown (protein for MGC:34025)
16.83333	15.58333	Homo sapiens, clone IMAGE:4838843, mRNA
16.81818	0.727273	Hs.97977 /UG_TITLE=ESTs
16.75556	4.377778	Homo sapiens mRNA; cDNA DKFZp586O2023 (from clone DKFZp586O2023)
16.66667	17.75	Hs.36409.0 /TIER=ConsEnd /STK=4 /UG=Hs.36409 /UG_TITLE=ESTs
16.65789	11.65789	Human hepatocyte nuclear factor-6 alpha (HNF6) mRNA, complete cds
16.625	3.5	Hs.188950 /UG_TITLE=ESTs
16.625	11.0625	Hs.277419 /UG_TITLE=ESTs
16.61111	12.77778	pancreatic ribonuclease (human, mRNA Recombinant Partial, 491 nt)
16.54545	15.09091	Homo sapiens, clone IMAGE:5277680, mRNA, partial cds.
16.53488	3.860465	Homo sapiens glutamate receptor, ionotrophic, AMPA 4 (GRIA4), mRNA. /PROD=glutamate receptor, ionotrophic /FL=gb:U16129.1 gb:NM_0
16.46575	11.61644	endothelin receptor type A /FL=gb:NM_001957.1 gb:L06622.1
16.42857	4.761905	Hs.99472 /UG_TITLE=ESTs
16.42105	5.631579	Homo sapiens mRNA for type I keratin. /PROD=HHa5 hair keratin type I intermediate filament
16.40909	3.227273	Homo sapiens protein tyrosine phosphatase, receptor-type, Z polypeptide 1 (PTPRZ1), mRNA
16.36	22.4	Homo sapiens neuropeptide Y receptor Y5 (NPY5R), mRNA
16.2	48.8	Homo sapiens cDNA: FLJ20890 fis, clone ADKA03323.
16.05882	3.882353	syntaphilin
16	13.5	Human DNA sequence from clone RP4-545L17 on chromosome 20p12.2-13. Contains the 5 end of the gene for a novel protein similar to RAD21 (S. pom
15.95522	8.552239	Homo sapiens cDNA FLJ36177 fis, clone TESTI2026515.
15.91667	0.5	Hs.40840 /UG_TITLE=ESTs
15.89474	25.12281	Homo sapiens cDNA FLJ13602 fis, clone PLACE1010089, highly similar to Homo sapiens mRNA for
15.88235	1.156863	Human CB-4 transcript of unrearranged immunoglobulin V(H)5 gene /DEF=Human CLL-12 transcript of unrearranged immuno
15.875	18.5	Homo sapiens, clone IMAGE:4823434, mRNA
15.85185	1.888889	Hs.173596 /UG_TITLE=ESTs

FIG. 7—*Continued*.

HTLV-1 p30^{II}	HTLV-1 p30^{II}/TIP60$_{\Delta HAT}$	Gene or Sequence Identity
15.83333	3.944444	Homo sapiens GPBP-interacting protein 90 mRNA, complete cds
15.81481	0.888889	Homo sapiens, Similar to recombination activating gene 1, clone MGC:43321 IMAGE:5265661, mRNA, complete cds
15.72414	2.241379	Homo sapiens cDNA FLJ37001 fis, clone BRACE2008172.
15.71429	11.42857	Homo sapiens, Similar to RIKEN cDNA 4833427G06 gene, clone IMAGE:5561932, mRNA
15.6875	9.0625	Homo sapiens, clone IMAGE:4831108, mRNA
15.6875	0.78125	Homo sapiens, clone IMAGE:5295305, mRNA
15.63636	5.681818	Hs.98388 /UG_TITLE=ESTs
15.61538	11.11538	methyl-CpG binding domain protein 2
15.59677	267.7419	Hs.154993 /UG_TITLE=ESTs
15.54545	9.181818	Homo sapiens transmembrane phosphatase with tensin homology (TPTE), mRNA.
15.52632	10.31579	Hs.105620 /UG_TITLE=ESTs
15.42857	23.28571	Homo sapiens acetyl LDL receptor; SREC=scavenger receptor expressed by endothelial cells (SREC), mRNA. /PROD=acetyl LDL receptor; SR
15.36842	0.684211	Homo sapiens cDNA: FLJ21351 fis, clone COL02762
15.36364	1.454545	Homo sapiens cDNA FLJ30168 fis, clone BRACE2000750.
15.3	12.83333	Homo sapiens clone 148022 iduronate-2-sulfatase (IDS2) pseudogene, mRNA sequence
15.27027	3.324324	Homo sapiens microtubule-associated protein tau (MAPT), transcript variant 1, mRNA.
15.23077	12.15385	Homo sapiens, clone IMAGE:4830182, mRNA.
15.21429	2.642857	Homo sapiens mRNA; cDNA DKFZp434H0872 (from clone DKFZp434H0872).
15.21053	1.684211	Homo sapiens cDNA: FLJ22630 fis, clone HSI06250.
15.19231	11.76923	Homo sapiens H2B histone family, member N (H2BFN), mRNA
15.19048	1.47619	Homo sapiens cDNA FLJ11921 fis, clone HEMBB1000318.
15.16667	1.233333	Hs.168268 /UG_TITLE=ESTs, Moderately similar to A35969 heparin-binding growth factor receptor K-sam precursor (H.sapiens)
15.125	1.1875	Human EST clone 53125 mariner transposon Hsmar1 sequence
15.09375	4	Homo sapiens, clone MGC:47837 IMAGE:6046539, mRNA, complete cds. /PROD=Unknown (protein for MGC:47837)
15.07407	4.277778	Homo sapiens cDNA: FLJ21710 fis, clone COL10087.
15.06667	15.96667	Hs.143834 /UG_TITLE=ESTs
15.05128	5.512821	hypothetical protein FLJ20271 /FL=gb:NM_017734.1
15.02564	5.974359	Homo sapiens full length insert cDNA clone YP60H04
15.02326	11.44186	Homo sapiens calsyntenin-2 (CS2), mRNA. /PROD=calsyntenin-2
15	1.5	Hs.104572 /UG_TITLE=ESTs
14.9403	12.67164	Homo sapiens inhibin, beta C (INHBC), mRNA. /PROD=inhibin beta C subunit precursor
14.88462	11.82692	Homo sapiens cDNA FLJ10146 fis, clone HEMBA1003327
14.80851	15.65957	gb:AW451826 /DB_XREF=gi:6992602 /DB_XREF=UI-H-BI3-alk-e-07-0-UI.s1 /CLONE=IMAGE:2737236 /FEA=EST /CNT=8 /TID=Hs.258791.0 /TIER=ConsEnd /STK=4 /UG=Hs.258791 /UG_TITLE=ESTs
14.78788	5.348485	gb:BF590323 /DB_XREF=gi:11682647 /DB_XREF=nab22h10.x1 /CLONE=IMAGE:3266922 /FEA=EST /CNT=33 /TID=Hs.55256.0 /TIER=Stack /STK=30 /UG=Hs.55256 /UG_TITLE=ESTs
14.71154	0.442308	Homo sapiens, clone IMAGE:4815474, mRNA
14.69565	12.67391	Homo sapiens RAGE mRNA for advanced glycation endproducts receptor, complete cds.
14.65217	22.82609	Homo sapiens, clone MGC:10724, mRNA, complete cds. /PROD=Unknown (protein for MGC:10724)
14.64286	2.571429	Homo sapiens mRNA; cDNA DKFZp761D191 (from clone DKFZp761D191)
14.61538	1.307692	Hs.313876 /UG_TITLE=ESTs
14.53488	8.348837	CGI-67 protein
14.5	9.772727	Hs.132650 /UG_TITLE=ESTs
14.42857	1.619048	Hs.293685 /UG_TITLE=ESTs
14.41667	4.708333	Hs.143789 /UG_TITLE=ESTs
14.40909	5.181818	Homo sapiens cDNA FLJ13755 fis, clone PLACE3000363.
14.33333	2.888889	Hs.327117 /UG_TITLE=ESTs
14.29032	1.903226	Hs.161566 /UG_TITLE=ESTs
14.27778	1.055556	Homo sapiens, clone IMAGE:4778480, mRNA.
14.23077	15.84615	Homo sapiens, Similar to hypothetical protein FLJ22792, clone MGC:22933 IMAGE:4905554, mRNA, complete cds
14.20513	1	Hs.162565 /UG_TITLE=ESTs
14.14815	21.37037	Homo sapiens, Similar to sex comb on midleg-like 3 (Drosophila), clone MGC:25118 IMAGE:4509724, mRNA, complete cds.
14.14286	11.57143	Homo sapiens olfactory-like receptor JCG8 (JCG8) mRNA, complete cds. /PROD=olfactory-like receptor JCG8
14.1	15.3	Homo sapiens, clone IMAGE:5267701, mRNA
14.06667	5.15	Homo sapiens cDNA FLJ34667 fis, clone LIVER2000769. /DEF=Homo sapiens cDNA FLJ34667 fis, clone LIVER2000769.
14.05882	7.588235	major histocompatibility complex, class II, DR beta 3
14.05882	3.176471	Hs.125962 /UG_TITLE=ESTs
14.05833	6.35	Hs.293118 /UG_TITLE=ESTs
14.03896	13.66234	Hs.20726 /UG_TITLE=ESTs
14.02778	9.555556	Homo sapiens, clone MGC:14510, mRNA, complete cds. /PROD=Unknown (protein for MGC:14510)
14.02632	17.39474	Homo sapiens CD84 antigen (leukocyte antigen) (CD84), mRNA. /PROD=CD84 antigen (leukocyte antigen)
14	11.90909	Hs.296235 /UG_TITLE=ESTs
14	38.29412	prostate specific G-protein coupled receptor /DEF=Homo sapiens prostate specific G-protein coupled receptor gene, comple
14	22.2	Homo sapiens cystic fibrosis transmembrane conductance regulator isoform 36 (CFTR) mRNA, partial cds
13.97826	12.54348	Homo sapiens testis transcript Y 9 (TTY9) mRNA, complete cds
13.90625	0.9375	Hs.88450 /UG_TITLE=ESTs
13.9	1.1	Hs.20468 /UG_TITLE=ESTs
13.89474	3.421053	Homo sapiens cDNA: FLJ21618 fis, clone COL07487.
13.85294	2.352941	Homo sapiens fibroblast growth factor 20 (FGF20), mRNA
13.81818	3.136364	Homo sapiens mRNA; cDNA DKFZp761J1323 (from clone DKFZp761J1323).
13.80769	2.307692	Hs.407438 /UG_TITLE=neurogenic differentiation 1
13.78788	12.45455	Homo sapiens hypothetical protein FLJ12983 (FLJ12983), mRNA
13.7549	9.77451	Human DNA sequence from clone RP5-1184F4 on chromosome 20q11.1-11.23. Contains the 3 end of gene KIAA0978, two genes for novel proteins similar
13.73333	8.8	Hs.201420 /UG_TITLE=ESTs
13.71429	12.17857	Homo sapiens cDNA FLJ12573 fis, clone NT2RM4000979
13.7	23.3	Hs.244710 /UG_TITLE=ESTs
13.68293	5.585366	Homo sapiens tenascin R (restrictin, janusin) (TNR), mRNA. /PROD=tenascin R (restrictin, janusin)
13.66667	1.606061	Hs.99336 /UG_TITLE=ESTs
13.64045	9.280899	Homo sapiens testis-specific ankyrin motif containing protein (LOC56311), mRNA.

FIG. 7—*Continued*.

HTLV-1 p30^{II}	HTLV-1 p30^{II}/TIP60$_{\Delta HAT}$	Gene or Sequence Identity
13.61538	1.846154	Hs.130922 /UG_TITLE=Homo sapiens, Similar to likely ortholog of yeast ARV1, clone IMAGE:5265646, mRNA
13.59259	0.814815	olfactory receptor, family 2, subfamily M, member 4 /DEF=H.sapiens mRNA for TPCR100 protein.
13.57143	3.142857	Homo sapiens, clone IMAGE:4694422, mRNA.
13.55882	3.661765	Homo sapiens small intestine aquaporin mRNA, complete cds
13.55172	3.689655	Homo sapiens mRNA; cDNA DKFZp564I083 (from clone DKFZp564I083)
13.55172	1.448276	gb:H47594 /DB_XREF=gi:923646 /DB_XREF=yp75c01.s1 /CLONE=IMAGE:193248 /TID=Hs2.407314.1 /CNT=3 /FEA=mRNA /TIER=ConsEnd /STK=1 /UG=Hs.407314 /UG_TITLE=Homo sapiens full length insert cDNA clone YP75C01
13.53846	7.807692	Homo sapiens cDNA FLJ39005 fis, clone NT2RI2024496
13.52941	11.2549	gb:H46217 /DB_XREF=gi:922269 /DB_XREF=yo14h12.s1 /CLONE=IMAGE:177959 /FEA=EST /CNT=4 /TID=Hs.268805.0 /TIER=ConsEnd /STK=4 /UG=Hs.268805 /UG_TITLE=ESTs
13.5	8.535714	Hs.250113 /UG_TITLE=ESTs, Moderately similar to thyroid hormone receptor-associated protein complex component TRAP150 (H.sap
13.40909	9.863636	Homo sapiens, clone IMAGE:3933453, mRNA
13.36842	0.842105	Hs.28714 /UG_TITLE=ESTs
13.35714	1.357143	Homo sapiens, clone IMAGE:5266862, mRNA.
13.35135	12.81081	Hs.158937 /UG_TITLE=ESTs
13.35	1.65	Homo sapiens cDNA FLJ13136 fis, clone NT2RP3003139
13.33333	6.6	Homo sapiens non-coding RNA HANC
13.30769	7.410256	Hs.25046 /UG_TITLE=ESTs
13.29384	8.21327	Homo sapiens protein kinase C, alpha binding protein (PRKCABP), mRNA
13.2807	4.017544	Homo sapiens hypothetical protein FLJ10979 (FLJ10979), mRNA. /PROD=hypothetical protein FLJ10979
13.25	7.15	Homo sapiens full length insert cDNA clone YI41B09
13.24138	0.896552	Homo sapiens, clone IMAGE:4818264, mRNA
13.2381	10.2619	Homo sapiens, clone IMAGE:4824978, mRNA
13.23333	15.1	gb:AA776626 /DB_XREF=gi:2835960 /DB_XREF=ae86f02.s1 /CLONE=IMAGE:971067 /FEA=EST /CNT=12 /TID=Hs.62183.0 /TIER=ConsEnd /STK=1 /UG=Hs.62183 /UG_TITLE=ESTs
13.2	8	myelin oligodendrocyte glycoprotein /DEF=Human DNA sequence from clone RP11-145L22 on chromosome 6p21.32-22.2
13.18182	0.818182	Homo sapiens regulator of G-protein signalling 1 (RGS1), mRNA. /PROD=regulator of G-protein signalling 1
13.11111	12.11111	Homo sapiens clone HQ0202 PRO0202 mRNA, partial cds
13.09091	17.30303	cytoplasmic linker associated protein 2
13.09091	17.63636	H.sapiens AA1 mRNA
13.04762	1.380952	Homo sapiens, clone IMAGE:4825614, mRNA.
13	1.75	Human clone 23909 mRNA, partial cds. /PROD=unknown
13	1.657143	Homo sapiens cDNA FLJ12289 fis, clone MAMMA1001788
12.93333	11.66667	Homo sapiens mRNA for keratin associated protein 4.7 (KRTAP4.7 gene)
12.93103	0.413793	Hs.43052 /UG_TITLE=ESTs
12.92308	4.846154	Homo sapiens cDNA FLJ14152 fis, clone MAMMA1003089.
12.88	1.52	Hs.118342 /UG_TITLE=ESTs
12.86207	6.965517	Homo sapiens, clone IMAGE:4042783, mRNA.
12.84	11.68	Homo sapiens POU domain, class 4, transcription factor 2 (POU4F2), mRNA. /PROD=POU domain, class 4, transcription factor 2
12.83333	8.111111	Hs.190319 /UG_TITLE=ESTs
12.8	3.72	Hs.231951 /UG_TITLE=ESTs
12.8	9.766667	Homo sapiens olfactory receptor-like protein JCG3 (JCG3), mRNA
12.78947	1.263158	Homo sapiens, clone IMAGE:4413783, mRNA.
12.78788	1.181818	Homo sapiens, clone IMAGE:4800001, mRNA.
12.76923	2	Homo sapiens, clone IMAGE:4828930, mRNA.
12.76471	1.705882	Homo sapiens mRNA expressed only in placental villi, clone SMAP41
12.75	17.08333	Hs.259168 /UG_TITLE=ESTs
12.69565	17.47826	Homo sapiens hypothetical protein FLJ21272 (FLJ21272), mRNA
12.6875	7.333333	Hs.92955 /UG_TITLE=ESTs
12.67857	4.071429	hypothetical protein FLJ10024 /DEF=Homo sapiens cDNA FLJ13978 fis, clone Y79AA1001665.
12.66102	9.050847	Homo sapiens RNA binding motif protein, Y chromosome, family 2, member B (RBMY2B) mRNA. /PROD=RNA binding motif protein, Y chromos
12.61538	1.384615	Hs.127556 /UG_TITLE=ESTs
12.57576	9.636364	Hs.44736 /UG_TITLE=ESTs
12.55172	0.724138	hypothetical protein LOC285965 /DEF=Homo sapiens mRNA; cDNA DKFZp686O0656 (from clone DKFZp686O0656).
12.54839	7.709677	Hs.276363 /UG_TITLE=hypothetical protein LOC283112
12.53333	14.86667	RFPL1S /UG_TITLE=ret finger protein-like 1 antisense
12.50847	1.559322	Hs.98945 /UG_TITLE=ESTs
12.5	6.136364	Hs.213371 /UG_TITLE=ESTs
12.45946	7.297297	Homo sapiens, similar to hypothetical protein, clone MGC:27103 IMAGE:4831323, mRNA, complete cds.
12.42424	16.54545	Homo sapiens GLB2 gene, upstream regulatory region

FIG. 7. Numerous cellular target genes are transcriptionally activated by HTLV-1 p30^{II} in a TIP60-dependent or TIP60-independent manner. (A) 293A fibroblasts were transfected with a CβS empty vector control, CMV-HTLV-1 p30^{II} (HA), or with CMV-HTLV-1 p30^{II} (HA) and CMV-TIP60$_{\Delta HAT}$ (25). Total cellular RNAs were extracted using a QIAGEN RNeasy kit as recommended by the manufacturer, and microarray gene expression analyses were performed by the Oregon State University Center for Gene Research and Biotechnology using Affymetrix Human U133Plus 2.0 full-genomic chips. Transcriptional activation of cellular genes by HTLV-1 p30^{II} is expressed as activation (*n*-fold) relative to the empty CβS vector control. A Microsoft Excel graphical representation of cellular target genes transcriptionally activated by HTLV-1 p30^{II} is shown. TIP60-dependent genes were identified based upon their transcriptional repression in the presence of the trans-dominant-negative TIP60$_{\Delta HAT}$ mutant (25). (B) Graphical representation of cellular genes transcriptionally repressed by HTLV-1 p30^{II} in a TIP60-dependent or TIP60-independent manner. (C) A list of major target gene sequences transcriptionally activated by HTLV-1 p30^{II} as determined by Affymetrix microarray gene expression analyses. Gene sequences whose transactivation was significantly dependent on the TIP60 coactivator are boxed. Hs., *Homo sapiens*.

numerous cellular genes are also transcriptionally repressed as a result of HTLV-1 $p30^{II}$ expression (44). Results shown in Fig. 7B graphically represent cellular target genes transcriptionally repressed (with levels ranging between 2.5-fold to 125-fold transrepression) by HTLV-1 $p30^{II}$ (HA) (red lines). Effects of the trans-dominant-negative $TIP60_{\Delta HAT}$ mutant upon transcriptional repression by HTLV-1 $p30^{II}$ (HA) are indicated by green lines (Fig. 7B).

In Fig. 7C, we provide a representative list of the major target gene sequences that are transcriptionally activated by HTLV-1 $p30^{II}$ (HA) as determined by Affymetrix microarray gene expression analyses. TIP60-dependent gene sequences are shown in boxes. Transcriptional activation is expressed as activation (*n*-fold) relative to the empty CβS vector control. Numerous cellular genes were transcriptionally induced by HTLV-1 $p30^{II}$ (HA) in a TIP60-dependent or TIP60-independent manner, suggesting that $p30^{II}$ may participate in multiple, distinct transcription complexes (Fig. 7C). With respect to the potential role of HTLV-1 $p30^{II}$ in adult T-cell leukemogenesis, transcriptional activation of the following genes is of significant interest: myeloid cell nuclear differentiation 1 antigen (31.1-fold; TIP60 dependent), protocadherin 15 (26.1-fold; TIP60 dependent), human protein tyrosine phosphatase delta precursor (23.3-fold; TIP60 dependent), cadherin 11-like precursor (20.2-fold; TIP60 dependent), colony-stimulating factor 2 receptor beta (19.6-fold; TIP60 independent), human protein tyrosine phosphatase receptor type Z polypeptide (16.4-fold; TIP60 dependent), *Schizosaccharomyces pombe* RAD21-like protein (16-fold; TIP60 independent), human transmembrane phosphatase with tensin homology (15.5-fold; TIP60 independent), H2B histone family member N (15.1-fold; TIP60 independent), major histocompatibility complex class II DR beta 3 (14.0-fold; TIP60 dependent), human CD84 leukocyte antigen (14.0-fold; TIP60 independent), prostate-specific G protein-coupled receptor (14.0-fold; TIP60 independent), fibroblast growth factor 20 (13.8-fold; TIP60 dependent), protein kinase C alpha-binding protein (13.2-fold; TIP60 independent), regulator of G-protein-signaling 1 (13.1-fold; TIP60 dependent), cytoplasmic linker associated protein 2 (13.0-fold; TIP60 independent), POU domain 4 transcription factor 2 (12.8-fold; TIP60 independent), RNA-binding motif protein (RBMY2B) (12.6-fold; TIP60 independent). Robek et al. (62) have demonstrated that an infectious HTLV-1 molecular clone, ACH.$p30^{II}$, exhibits an approximately 20 to 50% reduction in transformation efficiency compared to the wild-type ACH.wt (62), suggesting that $p30^{II}$ is required for the full transforming potential of HTLV-1. Our microarray analyses indicate that numerous cellular genes are transcriptionally activated by $p30^{II}$, and proteins encoded by these genes may contribute to HTLV-1 leukemic transformation and development of ATLL.

HTLV-1 $p30^{II}$ enhances Myc transforming potential and requires the TIP60 HAT and TRRAP/p434. As the c-Myc oncogene is known to cause cellular transformation (7, 41, 51), we next investigated whether HTLV-1 $p30^{II}$ might influence Myc-associated transforming activity in focus formation assays using immortalized human $WRN^{-/-}$ fibroblasts, which lack Werner's syndrome helicase functions (45). This cellular background was chosen because ATLL is an aging-related malignancy requiring clinical latency periods of 25 to 40 years prior to disease onset (29), which suggests that genetic mutations linked to the aging process likely contribute to leukemogenesis. Werner's syndrome is a premature aging disorder (45) that mimics or recapitulates many of the clinical and cellular features of normal aging, and *WRN* locus (8p11-12) mutations have been found in HTLV-1-infected ATLL patient lymphocytes and in HTLV-1-infected mycosis fungoides/Sezary syndrome cells (4, 30, 53, 69, 82). Neither c-Myc nor HTLV-1 $p30^{II}$ (HA) alone significantly induces focus formation in immortalized human $WRN^{-/-}$ fibroblasts (Fig. 8A). Surprisingly, in combination, HTLV-1 $p30^{II}$ (HA)-Myc coexpression reproducibly induces between 35 and 58 foci in different assays (Fig. 8A and B). The expression of HTLV-1 $p30^{II}$ (HA) and c-Myc (FLAG) was detected in transformed colonies by immunofluorescence microscopy (Fig. 8D and E), and the $p30^{II}$ protein appeared to be distributed throughout the nucleoplasm (Fig. 8C). We also observed a high incidence of multinucleated giant cells in isolated HTLV-1 $p30^{II}$ (HA) Myc-transformed fibroblasts that were expanded in culture, consistent with HTLV-1 $p30^{II}$-induced polyploidy observed during BrdU-FACS analyses (Fig. 8F; compare to control cells in Fig. 8D). The expression of HTLV-1 $p30^{II}$ (HA) in transformed fibroblasts was confirmed by immunoblotting using a monoclonal anti-HA antibody (Fig. 8E). As expected, the majority of expanded HTLV-1 $p30^{II}$ (HA)-expressing colonies showed increased levels of intracellular Myc protein by immunoblotting (Fig. 8F). Indeed, these findings indicate that HTLV-1 $p30^{II}$ markedly enhances the transforming potential of c-Myc and may promote genomic instability, resulting in polyploidy.

Our transcriptional activation data suggested that enhancement of Myc functions by HTLV-1 $p30^{II}$ requires the coactivators TIP60 and TRRAP/p434. Therefore, we tested whether focus formation induced by coexpressing HTLV-1 $p30^{II}$ (HA)-Myc might be affected by overexpressing wild-type TIP60 or $TIP60_{\Delta HAT}$ and $TIP60_{L497A}$ mutant proteins (17, 25). Results from two independent experiments in Fig. 9A indicate that none of the TIP60 expression constructs, either alone or in combination with c-Myc, significantly induces focus formation in immortalized human $WRN^{-/-}$ fibroblasts. However, ectopic TIP60 markedly increases focus formation induced by HTLV-1 $p30^{II}$ (HA)-Myc coexpression (Fig. 9A). The trans-dominant-negative $TIP60_{\Delta HAT}$ mutant completely abrogated colony formation by HTLV-1 $p30^{II}$ (HA)-Myc, and the $TIP60_{L497A}$ mutant partially inhibited focus formation (Fig. 9A). Increased colony formation by HTLV-1 $p30^{II}$ (HA)/Myc/TIP60, compared to inhibition of focus formation by the trans-dominant-negative $TIP60_{\Delta HAT}$ mutant, is shown in Fig. 9B. Inhibition of TRRAP/p434, as a result of coexpressing increasing amounts of $TRRAP_{antisense}$ RNA (41), also significantly decreased focus formation by HTLV-1 $p30^{II}$ (HA)-Myc (Fig. 9C). These findings collectively agree with our transcriptional activation data and suggest that HTLV-1 $p30^{II}$ enhances Myc transcriptional and transforming activities in a TIP60 HAT- and TRRAP-dependent manner.

As we have mapped the TIP60-interacting domain of HTLV-1 $p30^{II}$ to amino acid residues 99 to 154 through biochemical GST pull-down experiments (see Fig. 5B), we next analyzed a naturally occurring truncation mutant of $p30^{II}$, HTLV-1 $p13^{II}$, which expresses the carboxyl terminus of $p30^{II}$, spanning from residue 155 to 241 (Fig. 10A) (1, 10, 34, 70). The $p13^{II}$ mutant lacks the TIP60-interacting region of $p30^{II}$ but

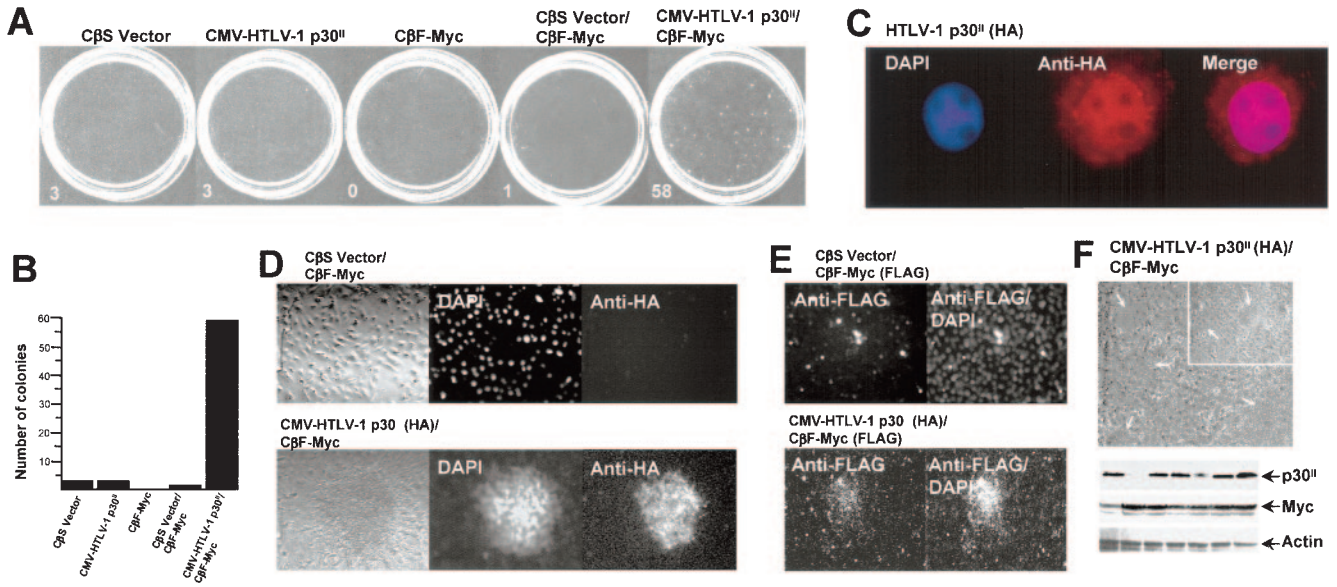

FIG. 8. HTLV-1 $p30^{II}$ enhances Myc-associated transforming potential. (A) Immortalized human $WRN^{-/-}$ fibroblasts (45) were transfected with CβS empty vector (3.0 μg), CMV-HTLV-1 $p30^{II}$ (HA) (3.0 μg), CβF-FLAG-Myc (3.0 μg), and combinations of CβS (1.5 μg)/CβF-FLAG-Myc (3.0 μg) or CMV-HTLV-1 $p30^{II}$ (HA) (1.5 μg)/CβF-FLAG-Myc (3.0 μg). Foci were quantified by direct counting, and representative results from triplicate experiments are shown. (B) Bar graph quantification of results shown in panel A. (C) HTLV-1 $p30^{II}$ (HA) was expressed throughout the nucleoplasm of HTLV-1 $p30^{II}$ (HA)/Myc-transformed fibroblasts. (D) CMV-HTLV-1 $p30^{II}$ (HA)/CβF-FLAG-Myc-transformed colonies and immortalized $WRN^{-/-}$ fibroblasts transfected with CβS/CβF-FLAG-Myc were stained with a monoclonal anti-HA tag antibody (CA5; Roche Molecular Biochemicals), rhodamine red-conjugated anti-mouse secondary antibody (Jackson ImmunoResearch Laboratories), and DAPI (Molecular Probes), and HTLV-1 $p30^{II}$ (HA) was detected by immunofluorescence microscopy. The c-Myc (FLAG) protein was visualized with transfected cells and transformed foci using a monoclonal anti-FLAG M2 antibody. (F) An increased number of multinucleated giant cells were observed in isolated HTLV-1 $p30^{II}$ (HA)/Myc-transformed $WRN^{-/-}$ fibroblasts expanded in culture. Expression of HTLV-1 $p30^{II}$ (HA), Myc, and actin proteins in expanded fibroblast cultures was detected by immunoblotting using monoclonal anti-HA, monoclonal anti-Myc, or goat polyclonal anti-actin antibodies.

contains the nuclear localization sequence as reported in references 1 and 34. Molt-4 lymphocytes were transfected with CMV-HTLV-1 $p30^{II}$ (HA), CMV-HTLV-1 $p13^{II}$ (HA), or a CβS empty vector control, and immunofluorescence microscopy was performed using an anti-HA (CA5) primary antibody and rhodamine red-conjugated fluorescent secondary antibody to visualize protein expression in transfected cells. The $p30^{II}$ (HA) and $p13^{II}$ (HA) proteins were observed in approximately 20 to 30% of transfected Molt-4 lymphocytes (Fig. 10B). We then analyzed BrdU incorporation and S-phase cell cycle progression in HTLV-1 $p30^{II}$ (HA)- or $p13^{II}$ (HA)-expressing transfected lymphoid cultures, compared to the CβS control. Results shown in Fig. 10C demonstrate that $p30^{II}$ (HA) expression markedly increased S-phase progression and polyploidy as noted in previous experiments (see Fig. 1D), whereas neither $p13^{II}$ (HA) nor the CβS control resulted in altered cell cycle progression (Fig. 10C).

To determine whether the TIP60-interacting domain (residues 99 to 154) of HTLV-1 $p30^{II}$ (HA) is essential for its oncogenic function, we compared the ability of $p30^{II}$ (HA) and $p13^{II}$ (HA) (corresponding to amino acids 155 to 241 of HTLV-1 $p30^{II}$) to promote focus formation in immortalized human $WRN^{-/-}$ fibroblasts in combination with c-Myc, as shown in Fig. 8A. These results demonstrate that the $p13^{II}$ (HA) mutant, lacking residues 1 to 154 of $p30^{II}$, is significantly defective for cellular transformation and focus formation compared to wild-type $p30^{II}$ (HA) (Fig. 10D), suggesting that TIP60 recruitment is required for $p30^{II}$-associated oncogenic activity. Finally, we tested the capacity of HTLV-1 $p30^{II}$ (HA) and $p13^{II}$ (HA) to transcriptionally activate the human cyclin D2 promoter-luciferase reporter construct in transfected 293A fibroblasts. Results shown in Fig. 10E demonstrate that $p13^{II}$ (HA), lacking the TIP60-interacting domain, is impaired for transcriptional-activating functions compared to $p30^{II}$ (HA), which transactivates the cyclin D2 promoter approximately eight- to ninefold. Indeed, $p13^{II}$ (HA) exhibited a trans-dominant-negative effect upon Myc-dependent transactivation from the cyclin D2 promoter and slightly repressed transcription below the basal level (Fig. 10E). Chromatin-immunoprecipitation analyses were performed with 293A fibroblasts expressing either HTLV-1 $p30^{II}$ (HA) or $p13^{II}$ (HA), by using antibodies against HTLV-1 $p30^{II}$ (the anti-HTLV-1 $p30^{II}$ or TofII antibody recognizes a peptide epitope within the COOH terminus of $p30^{II}$ that is also present in HTLV-1 $p13^{II}$ [32]), Myc, TIP60, TRRAP, TIP48, TIP49, and hGCN5. Immunoprecipitation products were amplified using the PRM primer pair, which anneals to nucleotide sequences flanking the conserved Myc-responsive E-box elements within the human cyclin D2 gene promoter (79). The $p30^{II}$ (HA) protein was precipitated in Myc-containing chromatin-remodeling complexes that contain TIP60, TRRAP, TIP48, TIP49, and hGCN5 (Fig. 10F, top panel). However, the $p13^{II}$ (HA) protein was not detected bound to Myc-responsive E-box elements within the cyclin D2 promoter and, consistent with $p13^{II}$'s transcriptional

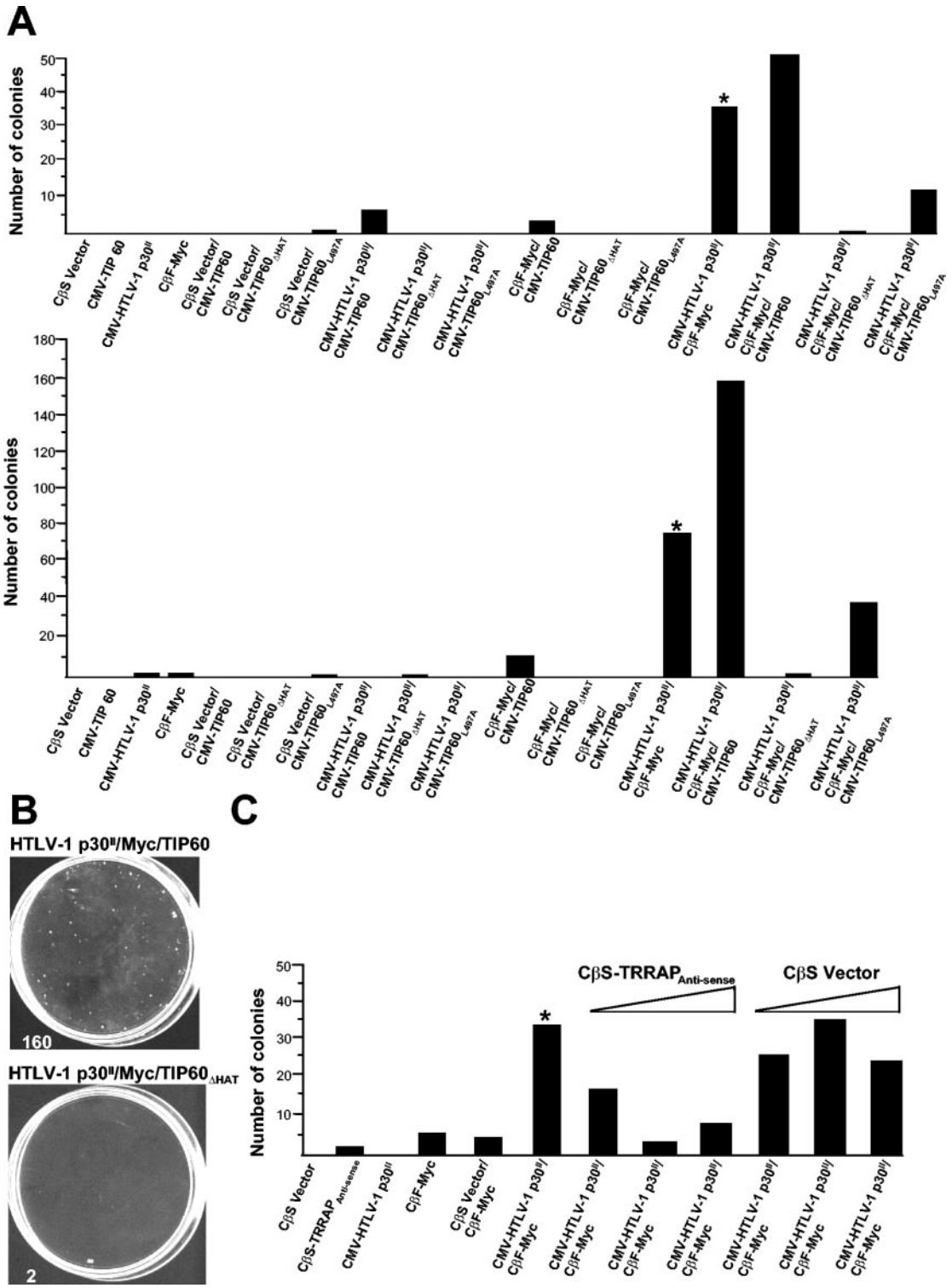

FIG. 9. HTLV-1 p30^{II}/Myc-transforming activity requires the transcriptional coactivators TIP60 and TRRAP/p434. (A) Immortalized human *WRN*$^{-/-}$ fibroblasts were transfected with CβF-FLAG-Myc (3.0 μg) and either CMV-HTLV-1 p30^{II} (HA) or empty CβS vector control (1.5 μg) in the presence of CMV-TIP60, CMV-TIP60$_{\Delta HAT}$, or CMV-TIP60$_{L497A}$ (3.0 μg), and focus formation/transformation assays were performed as described for Fig. 8A. Results from two independent experiments are shown for comparison. (B) Overexpression of wild-type TIP60 results in increased focus formation in *WRN*$^{-/-}$ fibroblasts cotransfected with CMV-HTLV-1 p30^{II} (HA), CβF-FLAG-Myc, and CMV-TIP60. Coexpression of the trans-dominant-negative TIP60$_{\Delta HAT}$ mutant (25) inhibits cellular transformation by HTLV-1 p30^{II} (HA)/Myc (lower panel). (C) Immortalized human *WRN*$^{-/-}$ fibroblasts were transfected as for panel A in the presence of increasing amounts of CβS-TRRAP$_{antisense}$ or CβS empty vector (0.5, 1.5, and 3.0 μg) and focus formation/transformation assays were performed (41). Colonies were quantified by direct counting, and representative results from duplicate experiments are shown. *, HTLV-1 p30^{II} (HA)/Myc focus formation.

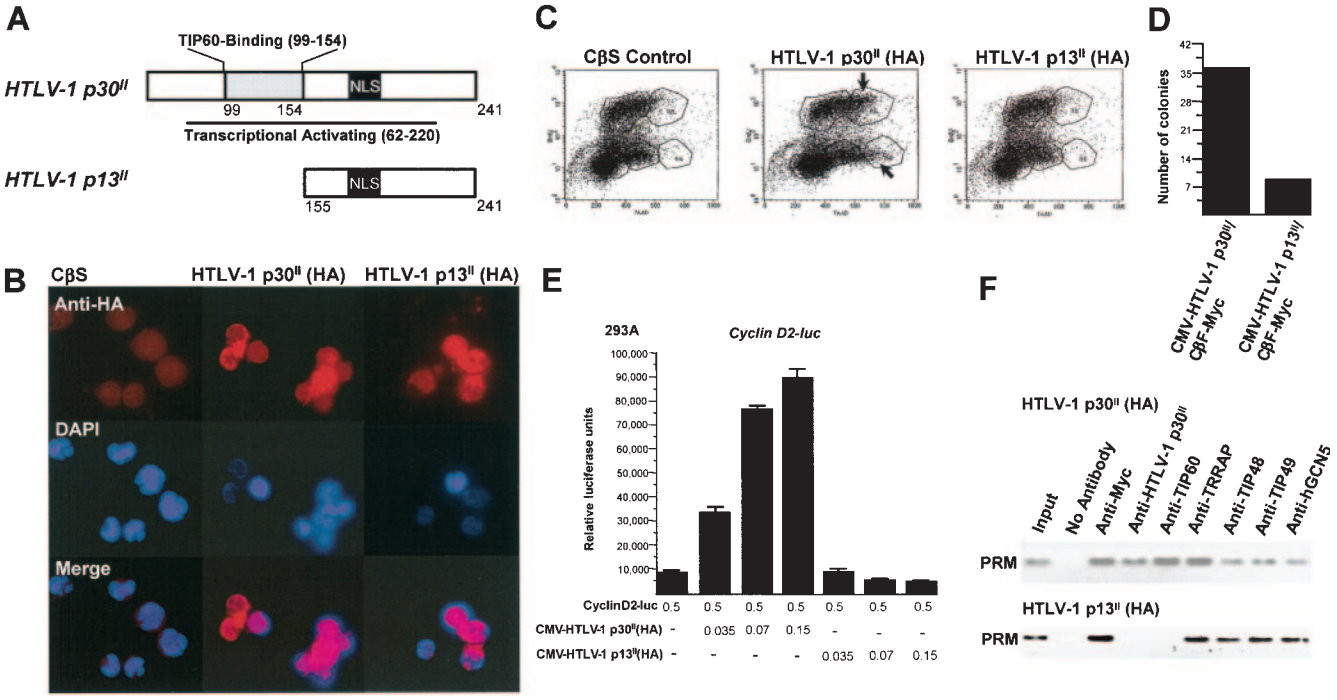

FIG. 10. An HTLV-1 $p30^{II}$-derived truncation mutant lacking the TIP60-interacting domain does not alter Myc-dependent transcription, cell cycle progression, or cellular transformation. (A) Diagram of HTLV-1 $p30^{II}$ and the naturally occurring truncation mutant $p13^{II}$, corresponding to amino acids 155 to 241 of $p30^{II}$ (1, 10, 34, 70). The TIP60-interacting region is located between amino acid residues 99 and 154, and the nuclear localization sequence (NLS) is depicted as described in reference 1. The transcriptional activating domain of HTLV-1 $p30^{II}$ has been previously mapped to residues 62 to 220 (1, 86, 87), which spans a region bearing significant amino acid sequence similarities to homeotic transcription factors, including Oct1, Pit1, and POU (1, 34). (B) Molt-4 lymphocytes were transfected with CMV-HTLV-1 $p30^{II}$ (HA), CMV-HTLV-1 $p13^{II}$ (HA), or a CβS control, and immunofluorescence microscopy was performed using a monoclonal anti-HA (CA5) primary antibody and rhodamine red-conjugated fluorescent secondary antibody (Jackson Laboratories). A DAPI nuclear staining is shown for reference. (C) Molt-4 lymphocytes were transfected as described for panel B, and cultures were analyzed for BrdU incorporation and total nuclear DNA content by FACS. Arrows indicate polyploid S-phase ($BrdU^+$; >2N nuclear content) and polyploid G_2/M ($BrdU^-$; 4N nuclear content) cell populations in $p30^{II}$ (HA)-expressing cultures. (D) Immortalized human *WRN*$^{-/-}$ fibroblasts were cotransfected with CMV-HTLV-1 $p30^{II}$ (HA)/CβF-Myc or CMV-HTLV-1 $p13^{II}$ (HA)/CβF-Myc, and focus formation assays were performed. Transformed colonies were observed after 2 weeks and quantified by direct counting. Representative results from duplicate experiments are shown. (E) 293A fibroblasts were cotransfected with a human cyclin D2 promoter-luciferase reporter construct (0.5 μg) in the presence of increasing amounts (0.07, 0.15, and 0.25 μg) of CMV-HTLV-1 $p30^{II}$ (HA) or CMV-HTLV-1 $p13^{II}$ (HA), and relative luciferase activities were determined using equivalent total cellular proteins. (F) Chromatin immunoprecipitation assays were performed by using 293A fibroblasts transfected with CMV-HTLV-1 $p30^{II}$ (top panel) or CMV-HTLV-1 $p13^{II}$ (bottom panel), with antibodies against HTLV-1 $p30^{II}$ (this antibody recognizes a peptide epitope within the COOH terminus of $p30^{II}$ and $p13^{II}$) (34), Myc, TIP60, TRRAP, TIP48, TIP49, and hGCN5. Precipitated oligonucleosomal DNA fragments, spanning conserved Myc-responsive E-box enhancer elements within the human cyclin D2 promoter, were amplified by PCR using the PRM oligonucleotide primer pair (79).

impairment, the TIP60 HAT was not present in Myc-containing cyclin D2 promoter complexes in the absence of $p30^{II}$ (HA) (Fig. 10F, lower panel). Our data suggest that the HTLV-1 $p30^{II}$ oncoprotein enhances Myc-dependent transcriptional and transforming activities through the stabilization of Myc-TIP60 interactions on promoters of Myc-responsive genes, which may also influence the acetylation of Myc protein by the TIP60 coactivator (Fig. 11) (56).

DISCUSSION

HTLV-1 infects $CD4^+$ T cells and promotes deregulated cell growth and lymphoproliferation associated with the development of ATLL. While numerous studies have demonstrated that the viral Tax protein transcriptionally activates growth/proliferative-signaling pathways, it has become increasingly evident that other pX-encoded regulatory factors ($p12^I$, $p13^{II}$, $p30^{II}$, Rex) are likely to perform essential functions during adult T-cell leukemogenesis (1, 6, 29, 34, 35, 48, 85). Indeed, the majority of partially deleted HTLV-1 proviruses in ATLL patient isolates contain intact pX sequences (33, 68), and alternatively spliced ORF I and ORF II mRNAs in HTLV-1-infected transformed T-cell lines and ATLL patient samples have been detected (6, 35). Cytotoxic T-lymphocytes specifically targeted against ORF I and ORF II peptides have been obtained from ATLL patients, suggesting that these proteins are present during in vivo HTLV-1 infections (57). Zhang et al. (86) reported that $p30^{II}$ interacts with p300/CREB-binding protein and represses Tax-mediated transactivation from the HTLV-1 LTR (86) and differentially modulates CREB-dependent transcription (87). Nicot et al. (48) and Younis et al. (85) have demonstrated that $p30^{II}$ prevents nuclear export of the doubly spliced Tax/Rex mRNA, and others have shown that $p30^{II}$ is required for maintenance of high viral titers in a rabbit model of ATLL using an infectious HTLV-1 molecular clone, ACH.30^{II}, which is defective for $p30^{II}$ production (5, 71). In-

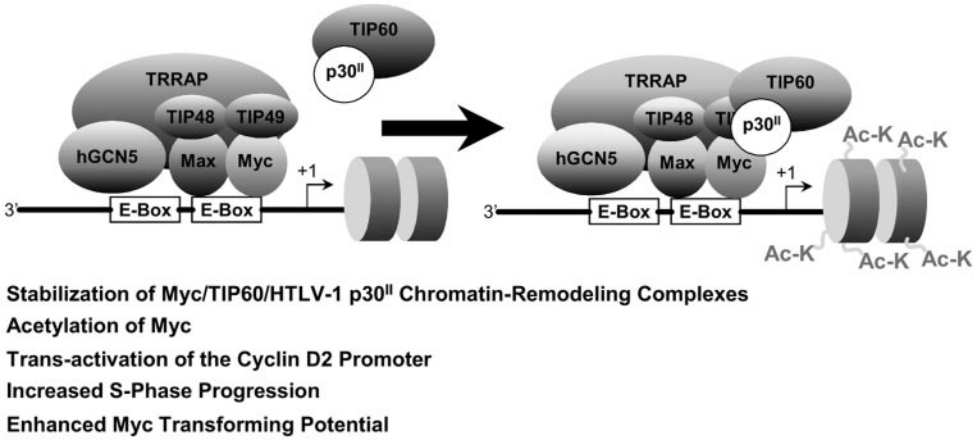

FIG. 11. Model of HTLV-1 $p30^{II}$ modulatory interactions with Myc-TIP60 transcription complexes assembled on E-box enhancer elements within promoters of Myc-responsive genes. Nucleosomal acetylation associated with transcriptional activation is indicated.

terestingly, Robek et al. (62) have previously demonstrated that $p30^{II}$ is dispensable for immortalization and transformation of human peripheral blood mononuclear cells by ACH.$p30^{II}$; however, this mutant exhibited an approximately 20 to 50% reduction in transformation efficiency compared to the wild-type ACH.wt (62), suggesting that $p30^{II}$ is required for the full transforming potential of HTLV-1. The physiological role of $p30^{II}$ in HTLV-1 pathogenesis remains unclear, and it is intriguing that, similar to Tax, $p30^{II}$ may perform multiple functions to control viral gene expression and promote deregulation of $CD4^+$ T-cell growth/proliferative pathways.

With this study, we have demonstrated that HTLV-1 $p30^{II}$ markedly enhances Myc-associated transcriptional and transforming activities and increases S-phase progression and polyploidy through interactions with the coactivator/HAT, TIP60 (Fig. 11). HTLV-1 $p30^{II}$ transactivates conserved E-box enhancer elements within promoters of Myc-responsive genes, requiring TIP60 HAT activity and the transcriptional coactivator TRRAP/p434. Frank et al. (16) have shown that preexisting Myc-TIP60 interactions contribute to Myc-dependent transcriptional activation and chromatin-remodeling associated with histone H4 acetylation on a subset of Myc-responsive genes in rodent and human fibroblasts, although their data suggest that Myc-TIP60 interactions may be relatively unstable on certain promoters. Patel et al. also recently demonstrated that c-Myc is a substrate for lysine acetylation by the TIP60 and hGCN5 acetyltransferases (56). Indeed, Myc and the TIP60 HAT likely exist in multiple distinct nuclear complexes, and Park et al. have demonstrated that TIP60 is not present in Myc/BAF53-containing transcription complexes (54). Our data indicate that, in absence of HTLV-1 $p30^{II}$-interactions, ectopic TIP60 overexpression does not significantly alter Myc transcriptional and transforming activities in functional assays (see Fig. 4A, 6C, and 9A). Further, we have shown that TIP60 is not detectably present in Myc-containing chromatin-remodeling complexes on the human cyclin D2 promoter (7, 79), in the absence of HTLV-1 $p30^{II}$, in uninfected Molt-4 lymphocytes (Fig. 5A). However, we did detect weak recruitment of TIP60 to Myc transcription complexes on the cyclin D2 promoter in pcDNA3.1–GFP-transfected 293A fibroblasts by ChIPs (Fig. 6B), consistent with the notion that Myc-TIP60 interactions may be relatively unstable on certain gene promoters. Thus, aberrant stabilization of Myc-TIP60 interactions, as a result of HTLV-1 $p30^{II}$ or other stabilizing factors, may contribute prominently to neoplastic transformation in hematological malignancies and solid tumors where Myc functions are deregulated or where *myc* locus mutations are present (18, 24, 26, 43, 55, 60).

The GST-HTLV-1 $p30^{II}$ protein interacts with both Myc and TIP60, and amino acid residues located between positions 99 and 154 of $p30^{II}$ interact with the TIP60 HAT in vivo. Recruitment of TIP60 is essential for $p30^{II}$-dependent effects upon cell cycle progression and focus formation/transformation. Affymetrix microarray gene expression analyses indicate that numerous cellular genes are transcriptionally activated by HTLV-1 $p30^{II}$ in a TIP60-dependent or TIP60-independent manner. These gene products could play important roles in HTLV-1-associated neoplastic disease. Our results indicate that HTLV-1 $p30^{II}$ is a novel retroviral enhancer of Myc-TIP60 transcriptional and transforming activities that may contribute to adult T-cell leukemogenesis.

ACKNOWLEDGMENTS

This work was supported by the Department of Biological Sciences, Southern Methodist University, Dallas, TX 75275-0376. B.L. acknowledges grant support from the Deutsche Forschungsgemeinschaft.

We thank G. Franchini (NCI, NIH) for generously providing CMV-HTLV-1 $p30^{II}$ (HA), CMV-HTLV-1 $p30^{II}$-GFP, and the anti-HTLV-1 $p30^{II}$ polyclonal antibody. We thank V. Ciminale (Department of Oncology and Surgical Sciences, University of Padua, Italy) for providing pSG-HTLV-1 $p13^{II}$ and C. Nicot (Department of Microbiology, Immunology and Molecular Genetics, University of Kansas) for providing CMV-HTLV-1 $p13^{II}$ (HA). We also thank J. K. Nyborg (Department of Biochemistry and Molecular Biology, Colorado State University) and R. S. Jones (Department of Biological Sciences, Southern Methodist University) for helpful comments and Carolyn K. Harrod for assistance in preparing the manuscript. Other members of the Harrod lab are thanked for their discussions and for critically reading the manuscript.

REFERENCES

1. **Albrecht, B., and M. D. Lairmore.** 2002. Critical role of human T-lymphotropic virus type 1 accessory proteins in viral replication and pathogenesis. Microbiol. Mol. Biol. Rev. **66:**396–406.

2. **Amati, B., and H. Land.** 1994. Myc-Max-Mad: a transcription factor network controlling cell cycle progression, differentiation, and death. Curr. Opin. Genet. Dev. **4:**102–108.
3. **Amati, B., T. D. Littlewood, G. I. Evan, and H. Land.** 1993. The c-Myc protein induces cell cycle progression and apoptosis through dimerization with Max. EMBO J. **12:**5083–5087.
4. **Assaf, C., M. Hummel, E. Dippel, S. Schwartz, C. C. Geilen, L. Harder, R. Siebert, M. Steinhoff, C. D. Klemke, E. Thiel, S. Goerdt, H. Stein, and C. E. Orfanos.** 2003. Common clonal T-cell origin in a patient with T-prolymphocytic leukemia and associated cutaneous T-cell lymphomas. Br. J. Haematol. **120:**488–491.
5. **Bartoe, J. T., B. Albrecht, N. D. Collins, M. D. Robek, L. Ratner, P. L. Green, and M. D. Lairmore.** 2000. Functional role of pX open reading frame II of human T- lymphotropic virus type I in maintenance of viral loads in vivo. J. Virol. **74:**1094–1100.
6. **Berneman, Z. N., R. B. Gartenhaus, M. S. Reitz, Jr., W. A. Blattner, A. Manns, B. Hanchard, O. Ikehara, R. C. Gallo, and M. E. Klotman.** 1992. Expression of alternatively spliced human T-lymphotropic virus type I pX mRNA in infected cell lines and in primary uncultured cells from patients with adult T-cell leukemia/lymphoma and healthy carriers. Proc. Natl. Acad. Sci. USA **89:**3005–3009.
7. **Bouchard, C., O. Dittrich, A. Kiermaier, K. Dohmann, A. Menkel, M. Eilers, and B. Lüscher.** 2001. Regulation of cyclin D2 gene expression by the Myc/Max/Mad network: Myc-dependent TRRAP recruitment and histone acetylation at the cyclin D2 promoter. Genes Dev. **15:**2042–2047.
8. **Cereseto, A., F. Diella, J. C. Mulloy, A. Cara, P. Michieli, R. Grassmann, G. Franchini, and M. E. Klotman.** 1996. p53 functional impairment and high p21waf1/cip1 expression in human T-cell lymphotropic/leukemia virus type I-transformed T cells. Blood **88:**1551–1560.
9. **Colgin, M. A., and J. K. Nyborg.** 1998. The human T-cell leukemia virus type 1 oncoprotein Tax inhibits the transcriptional activity of c-Myb through competition for the CREB binding protein. J. Virol. **72:**9396–9399.
10. **D'Agostino, D. M., L. Ranzato, G. Arrigoni, I. Cavallari, F. Belleudi, M. R. Torrisi, M. Silic-Benussi, T. Ferro, V. Petronilli, O. Marin, L. Chieco-Bianchi, P. Bernardi, and V. Ciminale.** 2002. Mitochondrial alterations induced by the p13II protein of human T-cell leukemia virus type 1. Critical role of arginine residues. J. Biol. Chem. **277:**34424–34433.
11. **Duyao, M. P., D. J. Kessler, D. B. Spicer, C. Bartholomew, J. L. Cleveland, M. Siekevitz, and G. E. Sonenshein.** 1992. Transactivation of the c-myc promoter by human T cell leukemia virus type 1 tax is mediated by NFκB. J. Biol. Chem. **267:**16288–16291.
12. **Evan, G. I., A. H. Wyllie, C. S. Gilbert, T. D. Littlewood, H. Land, M. Brooks, C. M. Waters, L. Z. Penn, and D. C. Hancock.** 1992. Induction of apoptosis in fibroblasts by c-myc protein. Cell **69:**119–128.
13. **Felber, B. K., H. Paskalis, C. Kleinman-Ewing, F. Wong-Staal, and G. N. Pavlakis.** 1985. The pX protein of HTLV-I is a transcriptional activator of its long terminal repeats. Science **229:**675–679.
14. **Fernandez, P. C., S. R. Frank, L. Wang, M. Schroeder, S. Liu, J. Greene, A. Cocito, and B. Amati.** 2003. Genomic targets of the human c-Myc protein. Genes Dev. **17:**1115–1129.
15. **Franchini, G., F. Wong-Staal, and R. C. Gallo.** 1984. Human T-cell leukemia virus (HTLV-I) transcripts in fresh and cultured cells of patients with adult T-cell leukemia. Proc. Natl. Acad. Sci. USA **81:**6207–6211.
16. **Frank, S. R., T. Parisi, S. Taubert, P. Fernandez, M. Fuchs, H. M. Chan, D. M. Livingston, and B. Amati.** 2003. MYC recruits the TIP60 histone acetyltransferase complex to chromatin. EMBO Rep. **4:**575–580.
17. **Gaughan, L., M. E. Brady, S. Cook, D. E. Neal, and C. N. Robson.** 2001. Tip60 is a co-activator specific for class I nuclear hormone receptors. J. Biol. Chem. **276:**46841–46848.
18. **Gavioli, R., T. Frisan, S. Vertuani, G. W. Bornkamm, and M. G. Masucci.** 2001. c-Myc overexpression activates alternative pathways for intracellular proteolysis in lymphoma cells. Nat. Cell Biol. **3:**283–288.
19. **Grandori, C., K. J. Wu, P. Fernandez, C. Ngouenet, J. Grim, B. E. Clurman, M. J. Moser, J. Oshima, D. W. Russell, K. Swisshelm, et al.** 2003. Werner syndrome protein limits MYC-induced cellular senescence. Genes Dev. **17:**1569–1574.
20. **Hall, A. P., J. Irvine, K. Blyth, E. R. Cameron, D. E. Onions, and M. E. Campbell.** 1998. Tumours derived from HTLV-I tax transgenic mice are characterized by enhanced levels of apoptosis and oncogene expression. J. Pathol. **186:**209–214.
21. **Haller, K., Y. Wu, E. Derow, I. Schmitt, K. T. Jeang, and R. Grassmann.** 2002. Physical interaction of human T-cell leukemia virus type 1 Tax with cyclin-dependent kinase 4 stimulates the phosphorylation of retinoblastoma protein. Mol. Cell. Biol. **22:**3327–3338.
22. **Harrod, R., Y. L. Kuo, Y. Tang, Y. Yao, A. Vassilev, Y. Nakatani, and C. Z. Giam.** 2000. p300 and p300/cAMP-responsive element-binding protein associated factor interact with human T-cell lymphotropic virus type-1 Tax in a multi-histone acetyltransferase/activator-enhancer complex. J. Biol. Chem. **275:**11852–11857.
23. **Harrod, R., Y. Tang, C. Nicot, H. S. Lu, A. Vassilev, Y. Nakatani, and C. Z. Giam.** 1998. An exposed KID-like domain in human T-cell lymphotropic virus type 1 Tax is responsible for the recruitment of coactivators CBP/p300. Mol. Cell. Biol. **18:**5052–5061.
24. **Hoffman, B., A. Amanullah, M. Shafarenko, and D. A. Lieberman.** 2002. The proto-oncogene c-myc in hematopoietic development and leukemogenesis. Oncogene **21:**3414–3421.
25. **Ikura, T., V. V. Ogryzko, M. Grigoriev, R. Groisman, J. Wang, M. Horikoshi, R. Scully, J. Qin, and Y. Nakatani.** 2000. Involvement of the TIP60 histone acetyltransferase complex in DNA repair and apoptosis. Cell **102:**463–473.
26. **Inghirami, G., L. Macri, E. Cesarman, A. Chadburn, J. Zhong, and D. M. Knowles.** 1994. Molecular characterization of $CD30^+$ anaplastic large-cell lymphoma: high frequency of c-myc proto-oncogene activation. Blood **83:**3581–3590.
27. **Jiang, H., H. Lu, R. L. Schiltz, C. A. Pise-Masison, V. V. Ogryzko, Y. Nakatani, and J. N. Brady.** 1999. PCAF interacts with tax and stimulates tax transactivation in a histone acetyltransferase-independent manner. Mol. Cell. Biol. **19:**8136–8145.
28. **Jin, D. Y., F. Spencer, and K. T. Jeang.** 1998. Human T cell leukemia virus type 1 oncoprotein Tax targets the human mitotic checkpoint protein MAD1. Cell **93:**81–91.
29. **Johnson, J. M., R. Harrod, and G. Franchini.** 2001. Molecular biology and pathogenesis of the human T-cell leukaemia/lymphotropic virus type-1 (HTLV-1). Int. J. Exp. Pathol. **82:**135–147.
30. **Karenko, L., S. Sarna, M. Kahkonen, and A. Ranki.** 2003. Chromsomal abnormalities in relation to clinical disease in patients with cutaneous T-cell lymphoma: a 5-year follow-up study. Br. J. Dermatol. **148:**55–64.
31. **Kehn, K., L. Deng, C. De La Fuente, K. Strouss, K. Wu, A. Maddukuri, S. Baylor, R. Rufner, A. Pumfery, M. E. Bottazzi, and F. Kashanchi.** 2004. The role of cyclin D2 and p21/waf1 in human T-cell leukemia virus type 1 infected cells. Retrovirology **1:**6.
32. **Kehn, K., C. D. Fuente, K. Strouss, R. Berro, H. Jiang, J. Brady, R. Mahieux, A. Pumfery, M. E. Bottazzi, and F. Kashanchi.** 2005. The HTLV-I Tax oncoprotein targets the retinoblastoma protein for proteasomal degradation. Oncogene **24:**525–540. [Online.]
33. **Konishi, H., N. Kobayashi, and M. Hatanaka.** 1984. Defective human T-cell leukemia virus in adult T-cell leukemia patients. Mol. Biol. Med. **2:**273–283.
34. **Koralnik, I. J., J. Fullen, and G. Franchini.** 1993. The p12I, p13II, and p30II proteins encoded by human T-cell leukemia/lymphotropic virus type I open reading frames I and II are localized in three different cellular compartments. J. Virol. **67:**2360–2366.
35. **Koralnik, I. J., A. Gessain, M. E. Klotman, A. Lo Monico, Z. N. Berneman, and G. Franchini.** 1992. Protein isoforms encoded by the pX region of human T-cell leukemia/lymphotropic virus type I. Proc. Natl. Acad. Sci. USA **89:**8813–8817.
36. **Kwok, R. P., M. E. Laurance, J. R. Lundblad, P. S. Goldman, H. Shih, L. M. Connor, S. J. Marriott, and R. H. Goodman.** 1996. Control of cAMP-regulated enhancers by the viral transactivator Tax through CREB and the co-activator CBP. Nature **380:**642–646.
37. **Lemasson, I., N. J. Polakowski, P. J. Laybourn, and J. K. Nyborg.** 2004. Transcription regulatory complexes bind the human T-cell leukemia virus 5′ and 3′ long terminal repeats to control gene expression. Mol. Cell. Biol. **24:**6117–6126.
38. **Liang, M. H., T. Geisbert, Y. Yao, S. H. Hinrichs, and C. Z. Giam.** 2002. Human T-lymphotropic virus type 1 oncoprotein tax promotes S-phase entry but blocks mitosis. J. Virol. **76:**4022–4033.
39. **Liu, B., M. H. Liang, Y. L. Kuo, W. Liao, I. Boros, T. Kleinberger, J. Blancato, and C. Z. Giam.** 2003. Human T-lymphotropic virus type 1 oncoprotein tax promotes unscheduled degradation of Pds1p/securin and Clb2p/cyclin B1 and causes chromosomal instability. Mol. Cell. Biol. **23:**5269–5281.
40. **Lemoine, F. J., and S. J. Marriott.** 2001. Accelerated G_1 phase progression induced by the human T cell leukemia virus type I (HTLV-I) Tax oncoprotein. J. Biol. Chem. **276:**31851–31857.
41. **McMahon, S. B., H. A. Van Buskirk, K. A. Dugan, T. D. Copeland, and M. D. Cole.** 1998. The novel ATM-related protein TRRAP is an essential cofactor for the c-Myc and E2F oncoproteins. Cell **94:**363–374.
42. **McMahon, S. B., M. A. Wood, and M. D. Cole.** 2000. The essential cofactor TRRAP recruits the histone acetyltransferase hGCN5 to c-Myc. Mol. Cell. Biol. **20:**556–562.
43. **Mengle-Gaw, L., and T. H. Rabbitts.** 1987. A human chromosome 8 region with abnormalities in B cell, HTLV-1^+ T cell and c-myc amplified tumours. EMBO J. **6:**1959–1965.
44. **Michael, B., A. M. Nair, H. Hiraragi, L. Shen, G. Feuer, K. Boris-Lawrie, and M. D. Lairmore.** 2004. Human T lymphotropic virus type-1 p30II alters cellular gene expression to selectively enhance signaling pathways that activate T lymphocytes. Retrovirology **1:**39.
45. **Moser, M. J., A. S. Kamath-Loeb, J. E. Jacob, S. E. Bennett, J. Oshima, and R. J. Monnat, Jr.** 2000. WRN helicase expression in Werner syndrome cell lines. Nucleic Acids Res. **28:**648–654.
46. **Mulloy, J. C., T. Kislyakova, A. Cereseto, L. Casareto, A. LoMonico, J. Fullen, M. V. Lorenzi, A. Cara, C. Nicot, C. Giam, and G. Franchini.** 1998. Human T-cell lymphotropic/leukemia virus type 1 Tax abrogates p53-induced cell cycle arrest and apoptosis through its CREB/ATF functional domain. J. Virol. **72:**8852–8860.

47. **Neuveut, C., K. G. Low, F. Maldarelli, I. Schmitt, F. Majone, R. Grassmann, and K. T. Jeang.** 1998. Human T-cell leukemia virus type 1 Tax and cell cycle progression: role of cyclin D-cdk and p110Rb. Mol. Cell. Biol. **18:**3620–3632.
48. **Nicot, C., M. Dundr, J. M. Johnson, J. R. Fullen, N. Alonzo, R. Fukumoto, G. L. Princler, D. Derse, T. Misteli, and G. Franchini.** 2004. HTLV-1-encoded p30(II) is a post-transcriptional negative regulator of viral replication. Nat. Med. **10:**197–201.
49. **Nicot, C., and R. Harrod.** 2000. Distinct p300-responsive mechanisms promote caspase-dependent apoptosis by human T-cell lymphotropic virus type 1 Tax protein. Mol. Cell. Biol. **20:**8580–8589.
50. **Nicot, C., R. Mahieux, C. Pise-Masison, J. Brady, A. Gessain, S. Yamaoka, and G. Franchini.** 2001. Human T-cell lymphotropic virus type 1 Tax represses c-Myb-dependent transcription through activation of the NF-κB pathway and modulation of coactivator usage. Mol. Cell. Biol. **21:**7391–7402.
51. **Nikiforov, M. A., S. Chandriani, J. Park, I. Kotenko, D. Matheos, A. Johnsson, S. B. McMahon, and M. D. Cole.** 2002. TRRAP-dependent and TRRAP- independent transcriptional activation by Myc family oncoproteins. Mol. Cell. Biol. **22:**5054–5063.
52. **Ohtani, K., R. Iwanaga, M. Arai, Y. Huang, Y. Matsumura, and M. Nakamura.** 2000. Cell type-specific E2F activation and cell cycle progression induced by the oncogene product Tax of human T-cell leukemia virus type I. J. Biol. Chem. **275:**11154–11163.
53. **Pancake, B. A., D. Zucker-Franklin, and E. E. Coutavas.** 1995. The cutaneous T cell lymphoma, mycosis fungoides, is a human T-cell lymphotropic virus-associated disease. A study of 50 patients. J. Clin. Investig. **95:**547–554.
54. **Park, J., M. A. Wood, and M. D. Cole.** 2002. BAF53 forms distinct nuclear complexes and functions as a critical c-Myc-interacting nuclear cofactor for oncogenic transformation. Mol. Cell. Biol. **22:**1307–1316.
55. **Pasqualucci, L., P. Neumeister, T. Goosens, G. Nanjangud, R. S. Chaganti, R. Kuppers, and R. Dalla-Favera.** 2001. Hypermutation of multiple proto-oncogenes in B-cell diffuse large-cell lymphomas. Nature **412:**341–346.
56. **Patel, J. H., Y. Du, P. G. Ard, C. Phillips, B. Carella, C. J. Chen, C. Rakowski, C. Chatterjee, P. M. Lieberman, W. S. Lane, G. A. Blobel, and S. B. McMahon.** 2004. The c-Myc oncoprotein is a substrate of the acetyltransferases hGCN5/PCAF and TIP60. Mol. Cell. Biol. **24:**10826–10834.
57. **Pique, C., A. Ureta-Vidal, A. Gessain, B. Chancerel, O. Gout, R. Tamouza, F. Agis, and M. Dokhelar.** 2000. Evidence for the chronic in vivo production of human T cell leukemia virus type I Rof and Tof proteins from cyctotoxic T lymphocytes directed against viral peptides. J. Exp. Med. **191:**567–572.
58. **Pise-Masison, C. A., K. S. Choi, M. Radonovich, J. Dittmer, S. J. Kim, and J. N. Brady.** 1998. Inhibition of p53 transactivation function by the human T-cell lymphotropic virus type 1 Tax protein. J. Virol. **72:**1165–1170.
59. **Poiesz, B. J., F. W. Ruscetti, A. F. Gazdar, P. A. Bunn, J. D. Minna, and R. C. Gallo.** 1980. Detection and isolation of type C retrovirus particles from fresh and cultured lymphocytes of a patient with cutaneous T-cell lymphoma. Proc. Natl. Acad. Sci. USA **77:**7415–7419.
60. **Popescu, N. C., and D. B. Zimonjic.** 2002. Chromosome-mediated alterations of the MYC gene in human cancer. J. Cell. Mol. Med. **6:**151–159.
61. **Popovic, M., P. S. Sarin, M. Robert-Gurroff, V. S. Kalyanaraman, D. Mann, J. Minowada, and R. C. Gallo.** 1983. Isolation and transmission of human retrovirus (human T-cell leukemia virus). Science **219:**856–859.
62. **Robek, M. D., F. H. Wong, and L. Ratner.** 1998. Human T-cell leukemia virus type 1 pX-I and pX-II open reading frames are dispensable for the immortalization of primary lymphocytes. J. Virol. **72:**4458–4462.
63. **Saggioro, D., D. M. D'Agostino, and L. Chieco-Bianchi.** 1999. Analysis of Tax-expressing cell lines generated from HTLV-1 tax-transgenic mice: correlation between c-myc overexpression and neoplastic potential. Exp. Cell Res. **247:**525–533.
64. **Schmitt, I., O. Rosin, P. Rohwer, M. Gossen, and R. Grassmann.** 1998. Stimulation of cyclin-dependent kinase activity and G_1- to S-phase transition in human lymphocytes by the human T-cell leukemia/lymphotropic virus type 1 Tax protein. J. Virol. **72:**633–640.
65. **Seiki, M., S. Hattori, Y. Hirayama, and M. Yoshida.** 1983. Human adult T-cell leukemia virus: complete nucleotide sequence of the provirus genome integrated in leukemia cell DNA. Proc. Natl. Acad. Sci. USA **80:**3618–3622.
66. **Seiki, M., A. Hikikoshi, T. Taniguchi, and M. Yoshida.** 1985. Expression of the pX gene of HTLV-I: general splicing mechanism in the HTLV family. Science **228:**1532–1534.
67. **Semmes, O. J., J. F. Barret, C. V. Dang, and K. T. Jeang.** 1996. Human T-cell leukemia virus type I tax masks c-Myc function through a cAMP-dependent pathway. J. Biol. Chem. **271:**9730–9738.
68. **Shaw, G. M., M. A. Gonda, G. H. Flickinger, B. H. Hahn, R. C. Gallo, and F. Wong-Staal.** 1984. Genomes of evolutionarily divergent members of the human T-cell leukemia virus family (HTLV-I and HTLV-II) are highly conserved, especially in pX. Proc. Natl. Acad. Sci. USA **81:**4544–4548.
69. **Shohat, M., E. Hodak, H. Hannig, W. Bodemer, M. David, and B. Shohat.** 1999. Evidence for the cofactor role of human T-cell lymphotropic virus type 1 in mycosis fungoides and Sezary syndrome. Br. J. Dermatol. **141:**44–49.
70. **Silic-Benussi, M., I. Cavallari, T. Zorzan, E. Rossi, H. Hiraragi, A. Rosato, K. Horie, D. Saggioro, M. D. Lairmore, L. Willems, L. Chieco-Bianchi, D. M. D'Agostino, and V. Ciminale.** 2004. Suppression of tumor growth and cell proliferation by p13II, a mitochondrial protein of human T cell leukemia virus type 1. Proc. Natl. Acad. Sci. USA **101:**6629–6634.
71. **Silverman, L. R., A. J. Phipps, A. Montgomery, L. Ratner, and M. D. Lairmore.** 2004. Human T-cell lymphotropic virus type 1 open reading frame II-encoded p30II is required for in vivo replication: evidence of in vivo reversion. J. Virol. **78:**3837–3845.
72. **Sun, S. C., J. Elwood, C. Beraud, and W. C. Greene.** 1994. Human T-cell leukemia virus type I Tax activation of NF-κB/Rel involves phosphorylation and degradation of IκBα and RelA (p65)-mediated induction of the c-*rel* gene. Mol. Cell. Biol. **14:**7377–7384.
73. **Suzuki, T., J. I. Fujisawa, M. Toita, and M. Yoshida.** 1993. The transactivator tax of human T-cell leukemia virus type 1 (HTLV01) interacts with cAMP-responsive element (CRE) binding and CRE modulator proteins that bind to the 21-base-pair enhancer of HTLV-1. Proc. Natl. Acad. Sci. USA **90:**610–614.
74. **Suzuki, T., H. Hirai, J. Fujisawa, T. Fujita, and M. Yoshida.** 1993. A transactivator Tax of human T-cell leukemia virus type 1 binds to NF-κB p50 and serum response factor (SRF) and associates with enhancer DNAs of the NF-κB site and CArG box. Oncogene **8:**2391–2397.
75. **Suzuki, T., H. Hirai, and M. Yoshida.** 1994. Tax protein of HTLV-1 interacts with the Rel homology domain of NF-κB p65 and c-Rel proteins bound to the NF-κB binding site and activates transcription. Oncogene **9:**3099–3105.
76. **Suzuki, T., S. Kitao, H. Matsushime, and M. Yoshida.** 1996. HTLV-1 Tax protein interacts with cyclin-dependent kinase inhibitor p16INK4A and counteracts its inhibitory activity towards CDK4. EMBO J. **15:**1607–1614.
77. **Van Orden, K., H. A. Giebler, I. Lemasson, M. Gonzales, and J. K. Nyborg.** 1999. Binding of p53 to the KIX domain of CREB binding protein. A potential link to human T-cell leukemia virus, type I-associated leukemogenesis. J. Biol. Chem. **274:**26321–26328.
78. **Van Orden, K., J. P. Yan, A. Ulloa, and J. K. Nyborg.** 1999. Binding of the human T-cell leukemia virus Tax protein to the coactivator CBP interferes with CBP-mediated transcriptional control. Oncogene **18:**3766–3772.
79. **Vervoorts, J., J. M. Luscher-Firzlaff, S. Rottmann, R. Lilischkis, G. Walsemann, K. Dohmann, M. Austen, and B. Lüscher.** 2003. Stimulation of c-Myc transcriptional activity and acetylation by recruitment of the cofactor CBP. EMBO Rep. **4:**484–490.
80. **Wagner, S., and M. R. Green.** 1993. HTLV-I Tax protein stimulation of DNA binding of bZIP proteins by enhancing dimerization. Science **262:**395–399.
81. **Wood, M. A., S. B. McMahon, and M. D. Cole.** 2000. An ATPase/helicase complex is an essential cofactor for oncogenic transformation by c-Myc. Mol. Cell **5:**321–330.
82. **Yeh, S.-P., M.-T. Yu, K.-C. Chow, L.-Y. Lai, and C.-F. Chiu.** 2002. Novel clonal der(8)t(8;14)(p11;q11),del(9)(q13q22) and t(14;22) (q13;q13) in a patient with fulminant adult T-cell leukemia/lymphoma. Cancer Genet. Cytogenet. **139:**34–37.
83. **Yoshida, M., I. Miyoshi, and Y. Hinuma.** 1982. Isolation and characterization of retrovirus from cell lines of human adult T-cell leukemia and its implications in the disease. Proc. Natl. Acad. Sci. USA **79:**2031–2035.
84. **Yoshimura, T., J. Fujisawa, and M. Yoshida.** 1990. Multiple cDNA clones encoding nuclear proteins that bind to the tax-dependent enhancer of HTLV-1: all contain a leucine zipper structure and basic amino acid domain. EMBO J. **9:**2537–2542.
85. **Younis, I., L. Khair, M. Dundr, M. D. Lairmore, G. Franchini, and P. L. Green.** 2004. Repression of human T-cell leukemia virus type 1 and type 2 replication by a viral mRNA-encoded posttranscriptional regulator. J. Virol. **78:**11077–11083.
86. **Zhang, W., J. W. Nisbet, B. Albrecht, W. Ding, F. Kashanchi, J. T. Bartoe, and M. D. Lairmore.** 2001. Human T-lymphotropic virus type 1 p30(II) regulates gene transcription by binding CREB binding protein/p300. J. Virol. **75:**9885–9895.
87. **Zhang, W., J. W. Nisbet, J. T. Bartoe, W. Ding, and M. D. Lairmore.** 2000. Human T-lymphotropic virus type 1 p30(II) functions as a transcription factor and differentially modulates CREB-responsive promoters. J. Virol. **74:**11270–11277.
88. **Zhao, L. J., and C. Z. Giam.** 1992. Human T-cell lymphotropic virus type I (HTLV-I) transcriptional activator, Tax, enhances CREB binding to HTLV-I 21-base-pair repeats by protein-protein interaction. Proc. Natl. Acad. Sci. USA **89:**7070–7074.